LETTER

https://doi.org/10.1038/s41586-018-0810-y

Actively personalized vaccination trial for newly diagnosed glioblastoma

Norbert Hilf[1,26], Sabrina Kuttruff-Coqui[1,26], Katrin Frenzel[2], Valesca Bukur[2], Stefan Stevanović[3,4], Cécile Gouttefangeas[3,4,5], Michael Platten[6,7,8], Ghazaleh Tabatabai[3,4,9], Valerie Dutoit[10], Sjoerd H. van der Burg[5,11], Per thor Straten[5,12,13], Francisco Martínez-Ricarte[14], Berta Ponsati[15], Hideho Okada[16,17], Ulrik Lassen[18], Arie Admon[19], Christian H. Ottensmeier[20], Alexander Ulges[1], Sebastian Kreiter[2,5], Andreas von Deimling[6,7], Marco Skardelly[9], Denis Migliorini[10], Judith R. Kroep[11], Manja Idorn[12,13], Jordi Rodon[14,22], Jordi Piró[15], Hans S. Poulsen[18], Bracha Shraibman[19], Katy McCann[20], Regina Mendrzyk[1], Martin Löwer[2], Monika Stieglbauer[3,5], Cedrik M. Britten[2,5,23], David Capper[6,7,24], Marij J. P. Welters[5,11], Juan Sahuquillo[14], Katharina Kiesel[1], Evelyna Derhovanessian[2], Elisa Rusch[3,5], Lukas Bunse[6,7], Colette Song[1], Sandra Heesch[2], Claudia Wagner[1], Alexandra Kemmer-Brück[2], Jörg Ludwig[1], John C. Castle[2,25], Oliver Schoor[1], Arbel D. Tadmor[21], Edward Green[7,8], Jens Fritsche[1], Miriam Meyer[1], Nina Pawlowski[1], Sonja Dorner[1], Franziska Hoffgaard[1], Bernhard Rössler[1], Dominik Maurer[1], Toni Weinschenk[1], Carsten Reinhardt[1], Christoph Huber[2], Hans-Georg Rammensee[3,4], Harpreet Singh-Jasuja[1], Ugur Sahin[2], Pierre-Yves Dietrich[10] & Wolfgang Wick[6,7]*

Patients with glioblastoma currently do not sufficiently benefit from recent breakthroughs in cancer treatment that use checkpoint inhibitors[1,2]. For treatments using checkpoint inhibitors to be successful, a high mutational load and responses to neoepitopes are thought to be essential[3]. There is limited intratumoural infiltration of immune cells[4] in glioblastoma and these tumours contain only 30–50 non-synonymous mutations[5]. Exploitation of the full repertoire of tumour antigens—that is, both unmutated antigens and neoepitopes—may offer more effective immunotherapies, especially for tumours with a low mutational load. Here, in the phase I trial GAPVAC-101 of the Glioma Actively Personalized Vaccine Consortium (GAPVAC), we integrated highly individualized vaccinations with both types of tumour antigens into standard care to optimally exploit the limited target space for patients with newly diagnosed glioblastoma. Fifteen patients with glioblastomas positive for human leukocyte antigen (HLA)-A*02:01 or HLA-A*24:02 were treated with a vaccine (APVAC1) derived from a premanufactured library of unmutated antigens followed by treatment with APVAC2, which preferentially targeted neoepitopes. Personalization was based on mutations and analyses of the transcriptomes and immunopeptidomes of the individual tumours. The GAPVAC approach was feasible and vaccines that had poly-ICLC (polyriboinosinic-polyribocytidylic acid-poly-L-lysine carboxymethylcellulose) and granulocyte–macrophage colony-stimulating factor as adjuvants displayed favourable safety and strong immunogenicity. Unmutated APVAC1 antigens elicited sustained responses of central memory CD8$^+$ T cells. APVAC2 induced predominantly CD4$^+$ T cell responses of T helper 1 type against predicted neoepitopes.

Targeting of selected neoepitopes by vaccination in melanoma—a tumour type that has many mutations—has demonstrated high immunogenicity and signs of clinical efficacy[6,7]. However, only a minority of mutations is processed to HLA-presented neoepitopes that can be targeted by T cells[8–10]. For cancers with few mutations, this is likely to be a limitation for antigen-unspecific immunotherapies, such as checkpoint inhibitors, as these tumours may frequently lack sufficient amounts of targetable neoepitopes. Nonetheless, clinical and radiographic responses to checkpoint inhibitors have been observed in patients with glioblastoma that had a hypermutation phenotype[11,12], suggesting that glioblastoma is in principle susceptible to immunotherapy[13]. T cell responses to unmutated, overpresented antigens have similarly demonstrated encouraging clinical data in glioblastoma[14–16] and may perfectly supplement the targeting of neoepitopes to achieve broad anti-tumour responses.

To establish a warehouse of premanufactured, synthetic peptides directly available for 'off-the-shelf' formulation, unmutated HLA-presented antigens were identified from 30 glioblastoma specimens using the XPRESIDENT technology[17]; preferred antigens were either frequently overpresented[18] or tumour-exclusive, but with low prevalence on tumours. Finally, 33 HLA-A*02:01-binding and 26 HLA-A*24:02-binding peptides (predominantly 9 amino acids; Supplementary Table 1) were selected into the warehouse, favouring candidates with good immunogenicity (see Methods). To address for every GAPVAC-101 patient the relevance of each warehouse peptide as a tumour antigen, the HLA immunopeptidomes and transcriptomes of each individual tumour were characterized by mass spectrometry and microarray analysis, respectively (Fig. 1). Pre-vaccine T cell reactivity completed the dataset that was used to generate a patient-specific ranking of the warehouse peptides (Extended Data Fig. 1a–d). As an example, the peptide PTP-013 ranked high for patient 5: it showed tumour-specific overpresentation (Extended Data Fig. 1b) and mRNA overexpression of the source gene (Extended Data Fig. 1c). Pre-vaccination peripheral blood mononuclear cells (PBMCs) of patient 5 contained CD8$^+$ T cells that were specific to PTP-013—a prerequisite for a later immune response (Extended Data Fig. 1d). Actively Personalized Vaccines 1 (APVAC1) were then composed of the seven best-ranking HLA class I peptides, two peptides binding promiscuously to different HLA-DR (class II) molecules ('pan-DR' antigens) and a viral marker peptide (Extended Data Fig. 2a). All APVAC1 compositions were different

[1]Immatics Biotechnologies GmbH, Tübingen, Germany. [2]BioNTech AG, Mainz, Germany. [3]Eberhard Karls Universität Tübingen, Tübingen, Germany. [4]German Cancer Consortium (DKTK), German Cancer Research Center Partner Site Tübingen, Tübingen, Germany. [5]CIMT/CIP - Association for Cancer Immunotherapy, working group Cancer Immunoguiding Program, Mainz, Germany. [6]University Hospital Heidelberg, Heidelberg, Germany. [7]German Cancer Consortium (DKTK), German Cancer Research Center, Heidelberg, Germany. [8]Medical Faculty Mannheim, Mannheim, Germany. [9]University Hospital Tübingen, Tübingen, Germany. [10]Geneva University Hospital, Geneva, Switzerland. [11]Leiden University Medical Center, Leiden, The Netherlands. [12]Center for Cancer Immune Therapy (CCIT), Department of Hematology, University Hospital Herlev, Herlev, Denmark. [13]Department of Immunology and Microbiology, University of Copenhagen, Copenhagen, Denmark. [14]Vall d'Hebron University Hospital, Barcelona, Spain. [15]BCN Peptides SA, Barcelona, Spain. [16]University of California, San Francisco, San Francisco, CA, USA. [17]Parker Institute for Cancer Immunotherapy, San Francisco, CA, USA. [18]Ringhospitalet, Copenhagen, Denmark. [19]Technion - Israel Institute of Technology, Haifa, Israel. [20]University of Southampton, Southampton, UK. [21]TRON GmbH - Translational Oncology at the University Medical Center of Johannes Gutenberg University, Mainz, Germany. [22]Present address: M. D. Anderson Cancer Center, University of Texas, Houston, TX, USA. [23]Present address: Oncology R&D, GlaxoSmithKline, Stevenage, UK. [24]Present address: Charité, University Medicine Berlin, Berlin, Germany. [25]Present address: Agenus Inc., Lexington, KY, USA. [26]These authors contributed equally: Norbert Hilf, Sabrina Kuttruff-Coqui. *e-mail: wolfgang.wick@med.uni-heidelberg.de

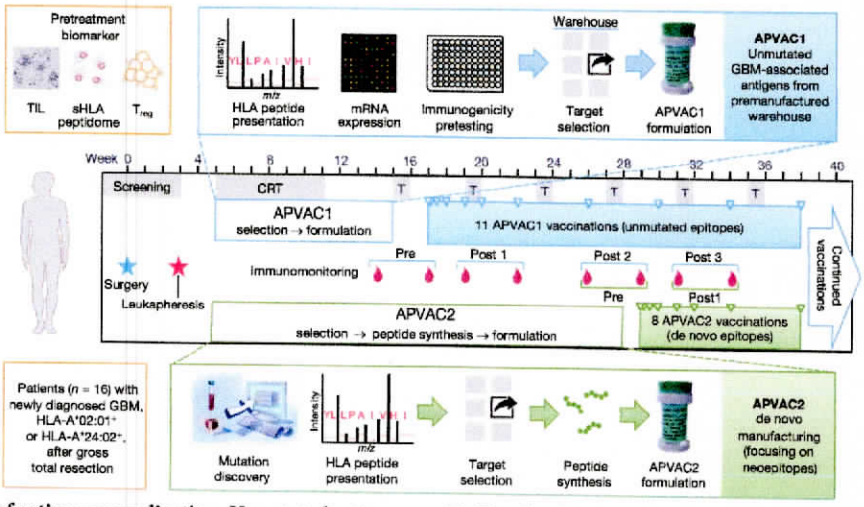

Fig. 1 | GAPVAC concept of active personalization. Unmutated antigens (APVAC1) and preferentially mutated, de novo antigens (APVAC2) were targeted. Vaccinations (triangles) in the GAPVAC-101 trial are superimposed on standard chemoradiotherapy (CRT) and maintenance TMZ cycles (T). Several pretreatment biomarkers and immune response data were evaluated. The soluble HLA (sHLA) analysis has previously been described[27]. GBM, glioblastoma.

($n = 16$; Supplementary Table 2), also illustrated by the selection frequencies of HLA-A*02:01 warehouse peptides for HLA-A*02:01$^+$ patients ($n = 13$; Extended Data Fig. 1e), supporting the warehouse concept for personalization. Median definition time from enrolment to start of APVAC1 manufacturing was 52 (range 42–74) days, and median production time until release of APVAC1 was 41 (33–51) days, enabling the planned vaccination start during the first maintenance temozolomide (TMZ) cycle.

For APVAC2, one of the following strategies was applied to select two peptides for good manufacturing practice (GMP) synthesis and to formulate the vaccine (Extended Data Figs. 1f, 2a). In the first strategy, mutation-containing peptides were confirmed as HLA ligands by mass spectrometry. In the second strategy, mutation-containing peptides with a predicted high likelihood for HLA class I binding and immunogenicity (usually peptides with a length of 19 amino acids with the mutation at position 10) were used; however, these were not confirmed by mass spectrometry to be HLA ligands. Finally, if neither of the two strategies identified suitable neoepitopes, unmutated glioblastoma-associated HLA class I epitopes that were identified in the individual immunopeptidome, but that were not part of the APVAC1 warehouse, were selected (9 to 10 amino acids). A median of 36 (19–84) somatic, non-synonymous mutations were detected by next-generation

Table 1 | Baseline characteristics and key outcomes for enrolled patients ($n = 16$)

Patient	Gender	Age	KPS	HLA	Non-synonymous mutations	MGMT promoter hypermethylated	Number of vaccinations (APVAC1/2)	Peptides vaccinated → immunogenic			OS (months)	PFS (months)
								APVAC1 class I	APVAC1 class II	APVAC2		
1	M	25	90	A*02:01	36	IR	10/7	7 → 4	2 → 1	M/N → 1	24.8[a]	22.2
2	F	48	80	A*02:01	35	–	13/10	7 → 3	2 → 1	M/N → 1	11.8	4.4
3	M	40	80	A*24:02	72	–	0/0	–	–	–	(8.7)	(8.7)
4	M	61	90	A*02:01	–	–	16/0	6 → 3	2 → 2	–	30.8	14.2
5	M	47	100	A*02:01	20	–	14/11	7 → 3	2 → 1	M/N → 0	26.7[a]	14.5
6	M	27	100	A*24:02	19	–	8/1	7 → 0	2 → 2	M/– → NE	29.0	17.9
7	F	35	80	A*02:01	23	–	14/10	7 → 3	2 → 2	M/M → 2	14.6	4.6
8	M	41	100	A*24:02	34	I	16/16	6 → 5	2 → 2	M/N → 2	38.9[a]	26.4
9	F	55	90	A*02:01 A*24:02	76	–	4/0	7 → NE	2 → NE	–	13.9	5.8
10	M	70	70	A*02:01	38	–	8/0	6 → 5	2 → 0	–	31.5[a]	30.4[a]
11	F	67	80	A*02:01	48	–	5/0	7 → NE	2 → NE	–	8.8	8.8
12	M	57	100	A*02:01	50	–	12/9	7 → 1	2 → 1	N/– → 0	19.3	10.8
13	F	50	90	A*02:01	38	NT	14/11	7 → 7	2 → 0	M/M → 2	16.9	5.3
14	F	70	90	A*02:01	84	+	12/8	6 → 5	2 → 0	M/M → 2	14.6	5.7
15	M	60	80	A*02:01	35	+	11/8	7 → 1	2 → 1	M/N → 1	34.1[a]	33.4[a]
16	F	57	90	A*02:01	35	+	16/15	7 → 5	2 → 0	M/M → 1	27.5[a]	27.4[a]
	F: 44% M: 56%	Median: 52.5 years	Median: 90	A*02:01$^-$: 81.3% A*24:02$^-$: 25%	Sum: 643 Median: 36 Mean: 43	28.6% MGMT hypermethylated	Median: 12/10 ($n = 15$/11)	92% immune responder ($n = 13$)	69% immune responder ($n = 13$)	80% immune responder ($n = 10$)	Median: 29.0 months ($n = 15$)	Median: 14.2 months ($n = 15$)

Patient 3 dropped out before first vaccination and was not included in analyses of overall and progression-free survival, although values are shown in parentheses. Tumour material from patient 4 was necrotic, therefore mutations could not be analysed. For patient 16, only one post-vaccination time point was evaluable for APVAC1 responses. 'APVAC2', the composition of vaccinated APVAC2 peptides (M, mutated antigen; N, unmutated antigen). IR, inconsistent results; KPS, Karnofsky Performance Score before first vaccination; MGMT, O^6-methylguanine-DNA methyltransferase; NE, not evaluable; NT, not tested; OS, overall survival from diagnosis; PFS, progression-free survival from diagnosis.
[a]Censored.

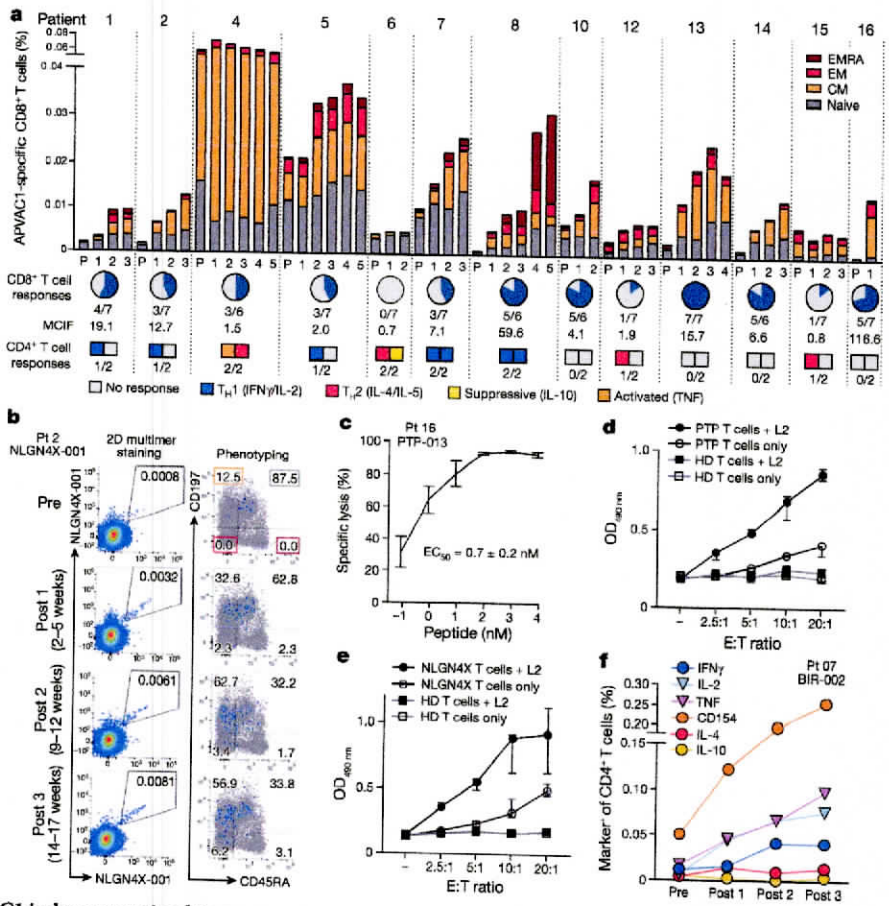

Fig. 2 | Unmutated APVAC1 induces sustained immune responses. **a**, Summary of immune responses to APVAC1 ($n = 13$ evaluable patients). Total APVAC1-specific CD8$^+$ T cell frequencies are shown. CM, central memory CD8$^+$ T cells; EM, effector memory CD8$^+$ T cells; EMRA, effector memory CD45RA$^+$ T cells; P, pretreatment samples; 1–5, post-treatment samples; MCIF, memory cell induction factor. For CD4$^+$ T cell responses, dominant phenotypes are indicated. **b**, CD8$^+$ T cell response in patient 2 against NLGN4X-001 evaluated pre- and post-treatment (Post 1–3). Percentages of specific CD8$^+$ T cells are indicated. Phenotyping: percentage of cells in the quadrants correspond to differentiation phenotypes (colour code as in **a**; see also Extended Data Fig. 4b). **c**, Avidity determination of PTP-013-reactive CD8$^+$ T cells from patient 16 (Vital-FR assay; effector:target (E:T) ratio = 10:1; data are mean ± s.d.; $n = 3$ replicates; flow cytometry data in Extended Data Fig. 3c). The half-maximal effective concentration (EC_{50}) ±s.e. is indicated. **d**, PTP T cells show cytotoxicity against the *PTPRZ1*$^+$ glioblastoma cell line L2. $OD_{490\,nm}$, optical density at 490 nm. **e**, NLGN4X T cells lysed *NLGN4X*$^+$ L2 cells. **d**, **e**, Lactate dehydrogenase release assays, $n = 3$ replicates; data are median ± range. HD T cells, healthy donor-derived T cells that are not target-specific. **f**, Response of CD4$^+$ T cells to the pan-DR peptide BIR-002 in patient 7 (flow cytometry data in Extended Data Fig. 5). For assays with limited patient materials, see 'Statistical analyses' in Methods.

sequencing within the analysed glioblastoma specimens from GAPVAC-101 patients (Table 1 and Supplementary Table 3). None of these 643 genomic mutations was identified in the HLA class I and II peptidomes of the respective patients ($n = 15$) by high-sensitivity mass spectrometry, whereas the same process identified a mutated HLA-presented peptide in another patient with hypermutated glioblastoma, but who did not participate in GAPVAC-101 (data not shown). Consequently, the selection of the two APVAC2 peptides was based on the second and third strategies presented above, preferring predicted, mutation-containing neoepitopes (Extended Data Fig. 1g). Eleven patients received APVAC2 compositions with a total of 20 de novo synthesized peptides (14 mutated and 6 unmutated; Extended Data Fig. 1h and Supplementary Table 4). Median definition time for APVAC2 was 96 (85–114) days and median production time was 86 (63–138) days.

APVAC1 and APVAC2 were applied independently by intradermal injections during TMZ maintenance therapy to HLA-A*02:01$^+$ or HLA-A*24:02$^+$ patients with newly diagnosed glioblastoma following gross total resection and standard chemoradiotherapy with TMZ (see Extended Data Fig. 2b for a detailed vaccination schedule). Granulocyte–macrophage colony-stimulating factor (GM-CSF) (intradermal injection) and poly-ICLC (subcutaneous injection) were co-applied as adjuvants and may enhance immune responses in a synergistic manner[19]. Clinical trial authorization (NCT02149225) was obtained in five European countries based on a standardized drug definition and GMP manufacturing process, leading to variable vaccine compositions for each patient (Extended Data Fig. 9c) and potentially serving as a model for future trials.

Primary end points were safety, tolerability, immunogenicity and operational feasibility of the concept. Of 58 screened patients (Extended Data Fig. 2e), 33 failed eligibility criteria and nine were not enrolled owing to limitations to the capacity of GMP production of peptides (1–2 patients per month). Sixteen patients were enrolled before entering chemoradiotherapy. Baseline characteristics of these patients reflect a standard population of patients with glioblastoma (Table 1). Fifteen patients received APVAC1 (median: 12 applications) and eleven patients received APVAC2 (median: 10 applications; Extended Data Fig. 2c).

All vaccinated patients experienced adverse events related to the drugs used in the study (Supplementary Table 5) that were within expectations. Mild-to-moderate injection site disorders were most frequent, consistent with the expected mechanism of action of the vaccinations. Eleven patients experienced adverse events of at least grade 3, mainly bone marrow suppression, which is frequently observed in patients who undergo chemoradiotherapy with TMZ. Two patients experienced an anaphylactic reaction after receiving vaccinations,

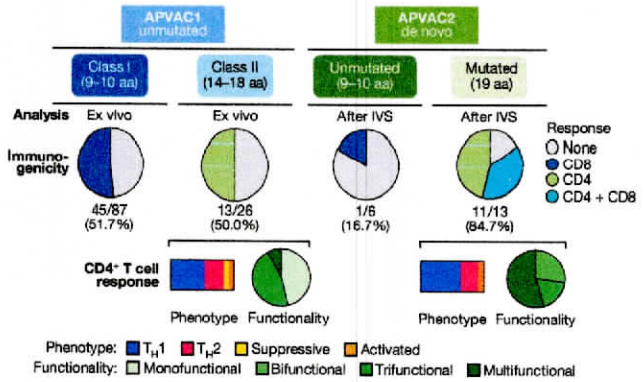

Fig. 3 | Summary of APVAC-induced responses. Typical amino acid (aa) lengths for APVAC peptide categories are indicated. IVS, in vitro sensitization.

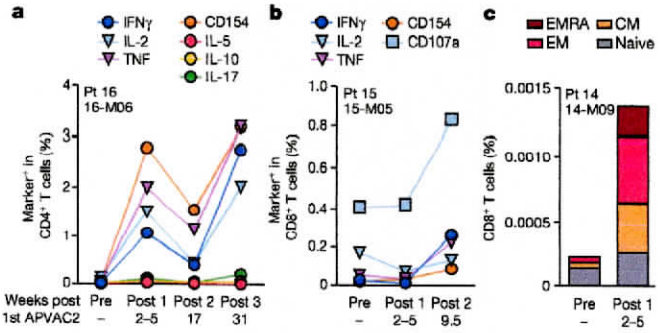

Fig. 4 | Neoepitope-targeting APVAC2 induces predominantly T_H1 CD4$^+$ T cell responses. a, Example T_H1 CD4$^+$ T cell response to mutated peptide 16-M06. **b**, Example CD8$^+$ T cell response to mutated peptide 15-M05. **a**, **b**, Pan-ICS after in vitro sensitization (flow cytometry data in Extended Data Fig. 6). **c**, CD8$^+$ T cell responses to a mutated epitope (HMKVSVYLL) contained in the 19-mer peptide 14-M09 (ex vivo 2D multimer assay, flow cytometry data in Extended Data Fig. 7b). For assays with limited patient materials, see 'Statistical analyses' in Methods.

potentially related to repeated application of GM-CSF[20]. Patient 9 required high-dose steroid treatment owing to potentially immune-associated grade 3 brain oedema.

Ex vivo multimer analysis revealed vaccine-induced CD8$^+$ T cell responses to at least one APVAC1 HLA class I peptide in 12 out of 13 patients (92.3%; median: 3 responses; Fig. 2a). These responses usually persisted for several months. The presence of specific precursor T cells in the blood of the patients was a strong selection criterion for APVAC1. Consequently, APVAC1-reactive T cells were frequently observed pre-vaccination, usually at a low frequency and with a naive phenotype. After vaccination, APVAC1-specific T cells shifted to a memory phenotype and in most cases showed an increased frequency (Fig. 2b). For single specificities, the magnitude of ex vivo measured CD8$^+$ T cell responses was up to 0.02% of CD8$^+$ T cells. The increase in expression of programmed cell death protein 1 (PD-1) was low to moderate, which is indicative of T cells that do not have an exhausted phenotype (Extended Data Fig. 3a, b). In total, 45 out of 87 (51.7%) vaccinated, immune-evaluable APVAC1 peptides were immunogenic (Figs. 2a, 3 and Supplementary Table 2).

APVAC1-induced PTP-013-reactive CD8$^+$ T cells cloned from post-vaccination PBMCs of patient 16 (PTP T cells) killed peptide-loaded K562-A2 target cells with high avidity (Fig. 2c and Extended Data Fig. 3d). These T cells also lysed the glioblastoma cell line L2 (Fig. 2d), which endogenously expresses the source gene of PTP-013 (*PTPRZ1*), demonstrating the functional capacities of APVAC1-induced T cells and the natural HLA presentation of PTP-013. The dominant NLGN4X-001-specific T cell receptor (TCR) from the same patient was cloned and re-expressed in PBMCs from a healthy donor. T cells transfected with this TCR (NLGN4X T cells) showed cytotoxicity against the cells of the NLGN4X$^+$ glioblastoma cell lines L2 (Fig. 2e) and P3XX (Extended Data Fig. 3e), whereas the cells of NLGN4X$^-$ glioblastoma cell line U87MG were only killed after transfection with *NLGN4X* (Extended Data Fig. 3f, g). In total, 9 out of 13 patients (69.2%) showed CD4$^+$ T cell responses to one or both unmutated pan-DR antigens in APVAC1 (ex vivo intracellular cytokine staining (ICS); example shown in Fig. 2f) with an overall immunogenicity of 50% for these peptides (Fig. 3). The responding T cells were of a heterogeneous phenotype, but frequently T helper type 1 (T_H1) cells (Figs. 2a, 3). The ratio of cumulative APVAC1-specific CD8$^+$ memory T cell frequencies post- compared to pre-vaccination for a patient was defined as the memory cell induction factor (MCIF) (Fig. 2a). The MCIF was higher in patients who lacked a predominant T_H2 or suppressive CD4$^+$ T cell response to APVAC1 (Extended Data Fig. 4d). Frequencies of regulatory T (T_{reg}) cell pre-vaccination (Extended Data Fig. 4a) were predictive of the biological activity of APVAC1. Low levels of T_{reg} cells were found in patients with a MCIF above median and were associated with a higher proportion of interferon-γ (IFN-γ)-producing APVAC1-specific CD4$^+$ T cells (Extended Data Fig. 4e, f).

Eight out of ten patients (80%) who were evaluable for APVAC2 immunogenicity developed neoepitope-specific, dominantly CD4$^+$ T cell responses (pan-ICS assay after in vitro sensitization; Extended Data Fig. 4h). In total, 11 out of 13 (84.7%) vaccinated, mutated APVAC2 peptides induced a CD4$^+$ T cell response (Figs. 3, 4a). These responses had predominantly a T_H1 phenotype and were multifunctional (Fig. 3). For two neoepitope-specific CD4$^+$ T cell responses, recognition of the corresponding wild-type sequences was tested, which revealed that one response showed cross-recognition and the other neoepitope specificity (Extended Data Fig. 7a), consistent with the broad spectrum of wild-type cross-recognition that has previously been reported[6]. Five neoepitope-specific CD4$^+$ T cell responses came with CD8$^+$ T cell responses to nested, mutated HLA class I-restricted epitopes (Fig. 4b and Extended Data Fig. 4h). None of the mutated APVAC2 peptides evoked an isolated CD8$^+$ T cell response. Notably, the 14-M09-specific CD8$^+$ T cell response measured by pan-ICS was confirmed by ex vivo multimer staining using a predicted, mutated HLA-A*02:01 ligand that was contained in the 19 amino acid-long peptide (Fig. 4c).

Figure 3 displays the favourable immunogenicity that was observed for GAPVAC-101. For the six unmutated antigens within APVAC2, an immune response was observed only once (patient 8). These antigens were immunized without prior knowledge about their immunogenicity (in contrast to APVAC1 peptides), arguing for the importance of immunogenicity as a selection criterion for HLA class I antigens.

Tumour-infiltrating lymphocytes (TILs) were isolated and cultured for all but one patient at initial surgery, applying a harmonized TIL isolation and expansion protocol for glioblastoma specimens (see Methods). Expanded TILs comprised CD4$^+$ and CD8$^+$ T cells (Extended Data Fig. 8a–c). Analysis of TCR clonotypes in tumours and corresponding expanded TIL cultures ($n = 3$) revealed relatively few amplified TCR clonotypes in glioma tissue, consistent with recent flow cytometry-based data[21] but in contrast to previous observations for TILs in other tumour types[22,23]. Notably, even fewer TCR clonotypes expanded in vitro (Extended Data Fig. 8d). No reactivity against any single APVAC was detected in any pre-vaccination TIL cultures from GAPVAC-101 patients or other patients with glioblastoma ($n = 30$ total, data not shown), suggesting that spontaneous T cell immunity against glioblastoma is rare but may be inducible by vaccination.

Some centrally confirmed radiographic responses were reported (Fig. 5a). However, in the months after chemoradiotherapy and maintenance TMZ such changes are seen frequently. Patients that received vaccinations ($n = 15$) had a median overall survival of 29.0 months from diagnosis and a median progression-free survival (PFS) of

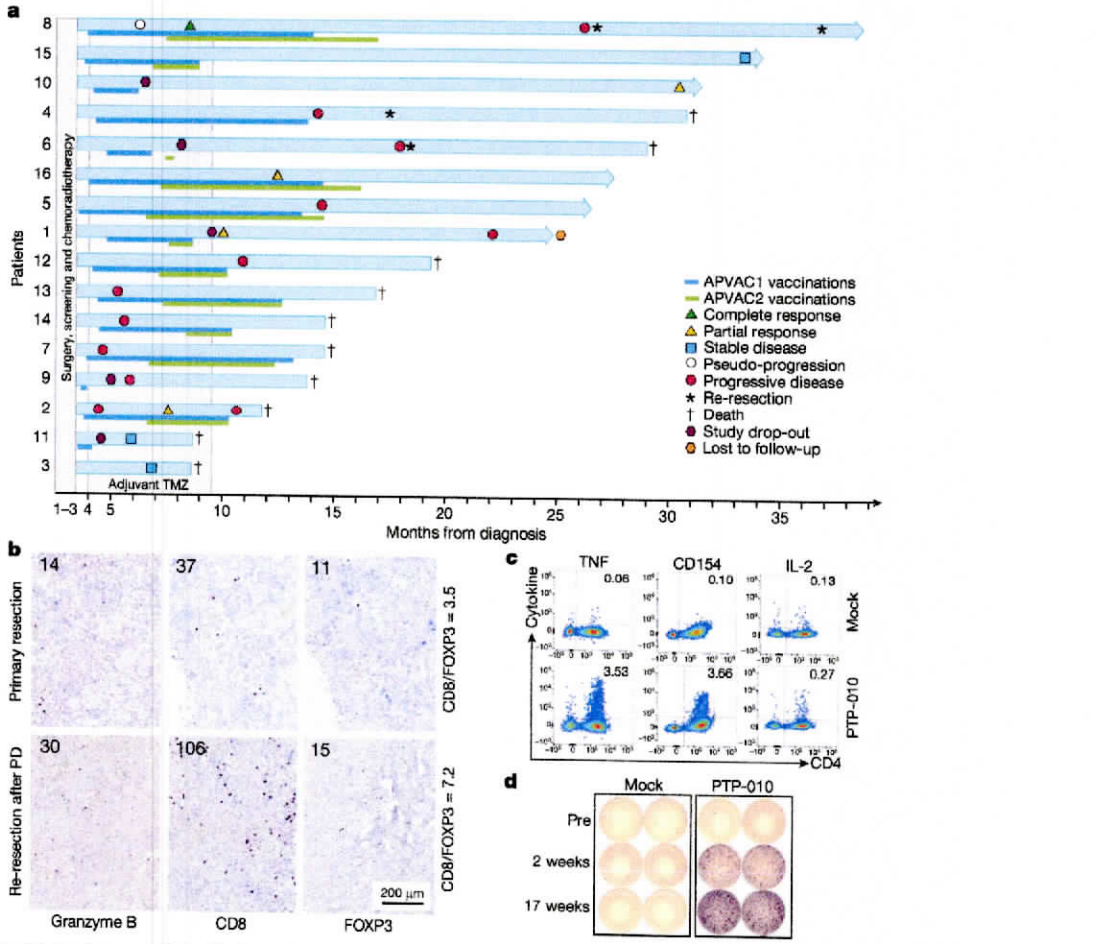

Fig. 5 | Clinical outcome and intratumoural T cells in patient 8. **a**, Swimmer plot for enrolled patients ($n = 16$). **b**, Immunohistochemical staining of tumour tissues from patient 8 for the primary tumour and at the first re-resection. The number of stained cells per mm^2 tumour tissue section are indicated ($n = 4$ independent regions analysed). **c**, **d**, CD4$^+$ T cell response against the APVAC1 pan-DR peptide PTP-010 in TIL at re-resection (**c**; ICS) and in PBMCs of patient 8 (**d**; IFNγ enzyme-linked immunospot assay; tested once in $n = 2$ replicates; for ICS data from PBMC, see Extended Data Fig. 4c). **c**, $n = 5$ independent experiments with 6 TIL cultures. Results provided from one of $n = 3$ positive cultures.

14.2 months (Extended Data Fig. 9a, b and Table 1). Patient 8, who had a resolved pseudo-progression and an overall survival of >38.9 months experienced a favourable immune response pattern, with CD8$^+$ T cell responses to five APVAC1 class I peptides, T_H1 CD4$^+$ T cell responses to both APVAC1 pan-DR peptides, and a combined CD8$^+$ and T_H1 CD4$^+$ T cell response to an APVAC2 neoepitope. The tumour was re-resected upon recurrence 26.8 months after diagnosis and demonstrated high infiltration by T cells with a favourable CD8$^+$ T/FOXP3$^+$ T_{reg} cell ratio (Fig. 5b). The tumour contained CD4$^+$ T cells directed against the APVAC1 pan-DR peptide PTP-010 (Fig. 5c), corresponding to multifunctional, T_H1-dominated reactivity in the periphery (Fig. 5d).

The warehouse-based APVAC1 process resulted in truly individual drug compositions, justifying the complex personalization. Failure to identify any of the 643 genomic mutations in the HLA peptidome of the patients may be due in part to the limited sensitivity of the mass spectrometry approach. However, rates below 1% were reported previously for the transition of mutations into HLA class I ligands[9,24], suggesting that the GAPVAC-101 data may partially reflect high attrition of mutations from the genetic level to actual HLA presentation of mutated peptides. This hypothesis is supported by the finding that during immunological validation of mutations, TILs were found to be reactive against only 1.2% of mutations[25]. Notably, the same mass spectrometry approach as applied here was able to identify mutated HLA ligands in human tumour tissue. With the uncertainty of neoepitope predictions, targeting of a higher number of mutations—if not all—would be favourable[8]. For glioblastoma and other tumour types that have low numbers of mutations, additional exploitation of the unmutated antigen pool is justified, and our personalized warehouse-based peptide vaccine approach was shown to be well-suited to address these antigens.

General superiority of neoepitopes to induce CD8$^+$ T cell responses versus unmutated class I peptides was not observed (Fig. 3), although data must be compared with caution since the peptide format, analysis methodology and availability of immunogenicity pretesting differed between APVAC1 and APVAC2. Our CD8$^+$ T cell reactivity compared favourably with previous trials and particularly with responses seen with a vaccine that shared several antigens with the GAPVAC warehouse[16] (Extended Data Fig. 4g). Improved immunogenicity may be attributable to the immune modulators, poly-ICLC plus GM-CSF (GAPVAC-101) versus GM-CSF alone (previous trial). Nevertheless, immune response induction needs further optimization.

The ACT IV trial, which tested rindopepimut with temozolomide for patients with newly diagnosed, EGFRvIII-expressing glioblastoma and had similar eligibility criteria, demonstrated a median overall survival of 20 months[26] and may come closest to a reference cohort, to which the median overall survival of 29 months of the GAPVAC-101 trial compares favourably with all limitations of comparing small early phase trials to phase III trials. Further efforts are required to decrease process complexity and duration, but the achievements of the current trial certainly warrant further studies to understand how anti-tumour immunity can be leveraged to ultimately achieve clinical benefit for patients with glioblastoma.

Online content

Any methods, additional references, Nature Research reporting summaries, source data, statements of data availability and associated accession codes are available at https://doi.org/10.1038/s41586-018-0810-y.

Received: 8 May 2018; Accepted: 19 November 2018;
Published online 19 December 2018.

1. Hodi, F. S. et al. Improved survival with ipilimumab in patients with metastatic melanoma. *N. Engl. J. Med.* **363**, 711–723 (2010).
2. Robert, C. et al. Nivolumab in previously untreated melanoma without *BRAF* mutation. *N. Engl. J. Med.* **372**, 320–330 (2015).
3. Snyder, A. et al. Genetic basis for clinical response to CTLA-4 blockade in melanoma. *N. Engl. J. Med.* **371**, 2189–2199 (2014).
4. Quail, D. F. & Joyce, J. A. The microenvironmental landscape of brain tumors. *Cancer Cell* **31**, 326–341 (2017).
5. Alexandrov, L. B. et al. Signatures of mutational processes in human cancer. *Nature* **500**, 415–421 (2013).
6. Sahin, U. et al. Personalized RNA mutanome vaccines mobilize poly-specific therapeutic immunity against cancer. *Nature* **547**, 222–226 (2017).
7. Ott, P. A. et al. An immunogenic personal neoantigen vaccine for patients with melanoma. *Nature* **547**, 217–221 (2017).
8. Schumacher, T. N. & Schreiber, R. D. Neoantigens in cancer immunotherapy. *Science* **348**, 69–74 (2015).
9. Yadav, M. et al. Predicting immunogenic tumour mutations by combining mass spectrometry and exome sequencing. *Nature* **515**, 572–576 (2014).
10. Freudenmann, L. K., Marcu, A. & Stevanović, S. Mapping the tumour human leukocyte antigen (HLA) ligandome by mass spectrometry. *Immunology* **154**, 331–345 (2018).
11. Bouffet, E. et al. Immune checkpoint inhibition for hypermutant glioblastoma multiforme resulting from germline biallelic mismatch repair deficiency. *J. Clin. Oncol.* **34**, 2206–2211 (2016).
12. Johanns, T. M. et al. Immunogenomics of hypermutated glioblastoma: a patient with germline *POLE* deficiency treated with checkpoint blockade immunotherapy. *Cancer Discov.* **6**, 1230–1236 (2016).
13. Platten, M., Bunse, L., Wick, W. & Bunse, T. Concepts in glioma immunotherapy. *Cancer Immunol. Immunother.* **65**, 1269–1275 (2016).
14. Okada, H. et al. Induction of $CD8^+$ T-cell responses against novel glioma-associated antigen peptides and clinical activity by vaccinations with α-type 1 polarized dendritic cells and polyinosinic-polycytidylic acid stabilized by lysine and carboxymethylcellulose in patients with recurrent malignant glioma. *J. Clin. Oncol.* **29**, 330–336 (2011).
15. Weller, M. et al. Vaccine-based immunotherapeutic approaches to gliomas and beyond. *Nat. Rev. Neurol.* **13**, 363–374 (2017).
16. Rampling, R. et al. A Cancer Research UK first time in human phase I trial of IMA950 (novel multi peptide therapeutic vaccine) in patients with newly diagnosed glioblastoma. *Clin. Cancer Res.* **22**, 4776–4785 (2016).
17. Weinschenk, T. et al. Integrated functional genomics approach for the design of patient-individual antitumor vaccines. *Cancer Res.* **62**, 5818–5827 (2002).
18. Dutoit, V. et al. Exploiting the glioblastoma peptidome to discover novel tumour-associated antigens for immunotherapy. *Brain* **135**, 1042–1054 (2012).
19. Morse, M. A. et al. Phase I study utilizing a novel antigen-presenting cell-targeted vaccine with Toll-like receptor stimulation to induce immunity to self-antigens in cancer patients. *Clin. Cancer Res.* **17**, 4844–4853 (2011).
20. Lawson, D. H. et al. Randomized, placebo-controlled, phase III trial of yeast-derived granulocyte–macrophage colony-stimulating factor (GM-CSF) versus peptide vaccination versus GM-CSF plus peptide vaccination versus placebo in patients with no evidence of disease after complete surgical resection of locally advanced and/or stage IV melanoma: a trial of the Eastern Cooperative Oncology Group-American College of Radiology Imaging Network Cancer Research Group (E4697). *J. Clin. Oncol.* **33**, 4066–4067 (2015).
21. Woroniecka, K. et al. T-cell exhaustion signatures vary with tumor type and are severe in glioblastoma. *Clin. Cancer Res.* **24**, 4175–4186 (2018).
22. Hadrup, S. R. et al. Tumor infiltrating lymphocytes in seminoma lesions comprise clonally expanded cytotoxic T cells. *Int. J. Cancer* **119**, 831–838 (2006).
23. Thor Straten, P. et al. Identification of identical TCRs in primary melanoma lesions and tumor free corresponding sentinel lymph nodes. *Cancer Immunol. Immunother.* **55**, 495–502 (2006).
24. Kalaora, S. et al. Use of HLA peptidomics and whole exome sequencing to identify human immunogenic neo-antigens. *Oncotarget* **7**, 5110–5117 (2016).
25. Tran, E. et al. Immunogenicity of somatic mutations in human gastrointestinal cancers. *Science* **350**, 1387–1390 (2015).
26. Weller, M. et al. Rindopepimut with temozolomide for patients with newly diagnosed, EGFRvIII-expressing glioblastoma (ACT IV): a randomised, double-blind, international phase 3 trial. *Lancet Oncol.* **18**, 1373–1385 (2017).
27. Shraibman, B. et al. Identification of tumor antigens among the HLA peptidomes of glioblastoma tumors and plasma. *Mol. Cell. Proteomics* **17**, 2132–2145 (2018).

Acknowledgements We thank all patients and their families for participating in this clinical trial; the Data Safety Monitoring Board (J. Rich, O. Chinot and C. Huber); S. Hess, M. Krauss (FGK) and S. Becker (spm²) for their contributions to trial management; I. Groskopf and M. Adis for technical support; T. Hillemann, M. Erdeljan and L. Alten for contributions to the revisions. A. Salazar (Oncovir) provided poly-ICLC. GAPVAC was supported by the European Union's FP7-HEALTH Research and Innovation funding program (number 305061). Further support information can be found in Supplementary Notes.

Reviewer information Nature thanks E. Jaffee, M. Lim and C. Melief for their contribution to the peer review of this work.

Author contributions C.M.B., C.H., H.-G.R., H.O., H.S.-J., J.C.C., N.H., O.S., S.K.-C., S.H., T.W., U.S. and W.W. developed the GAPVAC concept and trial design. D. Migliorini, F.M.-R., G.T., H.S.P., J.R.K., J.R., J.S., M. Skardelly, P.-Y.D., U.L. and W.W. recruited and treated patients. A.K.-B., B.R., C.R., J.L., K.F., M.M., N.H., N.P., P.-Y.D. and W.W overviewed the clinical trial conduct and assured compliance with Good Clinical Practice (GCP). A.v.D., A.D.T., C.S., D.C., J.C.C., J.F., K.F., M.L., N.H., O.S., S.H., S.K., S.K.-C., T.W. and V.B. contributed and/or evaluated data for the APVAC vaccines. B.P., H.-G.R., J.P., M. Stieglbauer, S.D. and S.S. contributed to APVAC manufacturing. A.U., C.G., C.W., D. Maurer, E.D., E.G., E.R., L.B., M.P., M.J.P.W., R.M., V.D. and W.W. contributed to immune response analyses. C.G., E.R., M.I., M.J.P.W., P.t.S., S.H.v.d.B. and V.D. contributed to the TIL analyses and together with C.M.B., G.T., M. Skardelly, J.R.K., H.S.P., P.-Y.D. and D. Migliorini contributed to the TIL protocol. A.A., A.U., B.S., C.H.O., K.M., K.F., R.M., U.S. and V.B. contributed further biomarker data. J.F., J.L., F.H., K.K., N.H., P.-Y.D., S.K.-C. and W.W. evaluated the clinical data. A.U., C.G., C.W., H.O., J.L., K.K., N.H., P.-Y.D., R.M., S.H.v.d.B., S.K.-C., V.D. and W.W. wrote the manuscript. A.D.T., C.S., J.F., K.F., M.L., N.H., O.S., S.H., S.K., S.K.-C., T.W. and V.B. contributed to Extended Data Fig. 1. A.U., C.W., D. Maurer and R.M. contributed to Fig. 2a–c, f, 3, 4 and Extended Data Figs. 1d, 3, 4a–c, 5, 6, 7b and 10. C.G., E.R. and H.-G.R. contributed to Fig. 5c, d and Extended Data Fig. 7a. V.D. and P.-Y.D. contributed to Extended Data Fig. 3d. M.P., L.B., E.G. and W.W. contributed to Fig. 2d, e and Extended Data Fig. 3e–g. K.M., A.U., R.M. and C.H.O. contributed to the T_{reg} cell data in Extended Data Fig. 4a, e, f. J.L., F.H., K.K., N.H., P.-Y.D. and W.W. contributed to Fig. 5a, Table 1, Extended Data Figs. 2, 9a, b and Supplementary Table 5. K.F., V.B. and U.S. contributed to Fig. 5b. C.G., E.R., M.I., M.J.P.W., P.t.S., S.H.v.d.B. and V.D. contributed to Extended Data Fig. 8.

Competing interests N.H., S.K.-C., A.U., R.M., K.K., C.W., J.L., O.S., J.F., M.M., N.P., S.D., F.H., D. Maurer, T.W., C.R. and H.S.-J. are employees of Immatics Biotechnologies. C.S. and B.R. contributed as former employees of Immatics to this work. T.W., C.R. and H.S.-J. are shareholders of Immatics. U.S., E.D., S.H., A.K.-B., K.F. and V.B. work for BioNTech. U.S. is CEO, co-founder and shareholder of BioNTech and inventor on patents related to personalized cancer immunotherapy. C.H. is co-founder, shareholder, advisor and member of the supervisory board of BioNTech AG, co-founder, advisor and member of the supervisory board of TRON AG. He also received honoraria from Immatics, Affiris, Abivax, Apceth, Suppremol and Vaxxim as member of advisory boards. M.L. works as a consultant and receives research funding from BioNTech and is co-inventor on patents related to the personalized cancer vaccine. A.D.T. is co-inventor on patents related to the personalized cancer vaccine. S.K. is vice president and advisor for BioNTech. C.M.B. contributed as former employee of BioNTech to this work. J.C.C. worked as an advisor for BioNTech. B.P. and J.P. are employees of BCN Peptides. H.-G.R. has received research grants from Boehringer-Ingelheim as well as honoraria from CureVac for advisory board participation and consulting for Navigo Proteins, AstraZeneca, MSD, BMS and MedImmune. C.G. has received research grants from Boehringer-Ingelheim and from RhoVac ApS. M.P. has received research grants from Bayer, Pfizer and Novartis as well as honoraria for lectures, advisory board participation or consulting from Bayer, Merck, Novartis, Roche, Affiris and Medac. G.T. has received research grants from Roche Diagnostics as well as honoraria for lectures, advisory board participation or consulting from Medac, BMS, Novocure and AbbVie. S.H.v.d.B. has received research grants from ISA Pharmaceuticals, Kite Pharma, Innate Pharma and IO-Biotech as well as honoraria for advisory board participation or consulting from ISA Pharmaceuticals, IO-Biotech, PCI Biotech, and GSK. P.t.S. has received honoraria from RhoVac. J.R. has received research grants from Bayer and Novartis as well as honoraria for lectures, advisory board participation or consulting from Novartis, Eli Lilly, Orion Pharmaceuticals, Servier Pharmaceuticals, Peptomyc, Merck Sharp & Dohme, Kelun Pharmaceutical/Klus Pharma and Spectrum Pharmaceuticals. H.O. has received research grants from Agios Pharmaceuticals, Ono Pharmaceutical as well as honoraria for lectures, advisory board participation or consulting from Bristol-Myers Squibb, Alexion Pharmaceuticals, Amal Therapeutics, Agios Pharmaceuticals and Eureka Therapeutics. J.R.K. has received research grants from Amgen, Astra Zeneca, Novartis, Sanofi and Philips as well as honoraria for lectures, advisory board participation or consulting from Amgen, Astra Zeneca, Eisai, Novartis, Pfizer, Roche and Tesaro. P.-Y.D. has received research grants from Immatics as well as honoraria for lectures, advisory board participation or consulting from BMS. W.W. has received research support from Apogenix, Boehringer Ingelheim, Pfizer, Roche and Vaximm. S.S., V.D., U.L., M.I., F.M.-R., C.H.O, H.S.P., A.v.D., J.S., M. Skardelly, D. Migliorini, A.A., B.S., E.R., M. Stieglbauer, D.C., L.B., E.G., K.M. and M.J.P.W. have no conflicts to disclose.

Additional information
Extended data is available for this paper at https://doi.org/10.1038/s41586-018-0810-y.
Supplementary information is available for this paper at https://doi.org/10.1038/s41586-018-0810-y.
Reprints and permissions information is available at http://www.nature.com/reprints.
Correspondence and requests for materials should be addressed to W.W.
Publisher's note: Springer Nature remains neutral with regard to jurisdictional claims in published maps and institutional affiliations.

METHODS

Data reporting. No statistical methods were used to predetermine sample size. The experiments were not randomized and the investigators were not blinded to allocation during experiments and outcome assessment.

APVAC1 warehouse. For the APVAC1 warehouse setup, immunopeptidomes of a total of 30 HLA-A*02$^+$ and HLA-A*24$^-$ glioblastoma tumour samples were analysed in 2012–2013 by mass spectrometry, revealing several thousands of different HLA-A*02:01- and HLA-A*24:02-presented peptides after applying the XPRESIDENT antigen discovery platform[17,28]. From this repertoire, strongly tumour-associated candidates were identified—that is, peptides that were exclusively found on tumours or were highly overpresented compared to the immunopeptidome of a panel of normal tissue types. Expression analyses of mRNAs from source genes of glioblastoma samples in comparison to expression in normal tissue and immunogenicity analysis of the blood of healthy donors was used as supportive data to select for 33 HLA-A*02:01 and 26 HLA-A*24:02 warehouse peptides (Supplementary Table 1).

GAPVAC-101 phase I trial design. Between 2014 and 2018, a single-arm, open-label first-in-human trial (NCT02149225) was conducted at six study centres in Germany, Switzerland, The Netherlands, Spain and Denmark in accordance with the Declaration of Helsinki, International Conference on Harmonization/GCP guidelines and all other applicable regulatory and ethical requirements. The trial was approved by the responsible Ethics Committees and regulatory agencies as described in the Supplementary Notes. All patients provided written informed consent. Patients were pseudoanonymized at the clinical centres. Patient identification logs were kept strictly confidential by the investigators. HLA-A*02:01$^-$ and/or HLA-A*24:02$^-$ patients with newly diagnosed glioblastoma after gross total resection as judged by a post-operative scan within 48 h post-surgery, Karnofsky performance score of $\geq$70% and a life expectancy of over six months were enrolled (see clinicaltrials.gov (https://clinicaltrials.gov/ct2/show/NCT02149225?cond=GAPVAC&rank=1) for details on eligibility criteria). From the initial surgery, a tumour tissue specimen was freshly frozen for later immunopeptidome, mRNA expression and mutanome analysis. If possible, a further tumour tissue sample was used fresh for isolation of TILs (see 'Functional testing of TILs'). Moreover, plasma samples were collected pre- and post-surgery for analysis of the soluble HLA ligandome[27]. Before the start of standard chemoradiotherapy with TMZ, leukapheresis was performed (target cell yield: 4.8×10^9 white blood cells) and PBMCs were isolated for analysis of the immune repertoire of individual patients (see below). APVAC1 and APVAC2 vaccines for each patient were designed and manufactured starting during standard-of-care chemoradiotherapy[29]. Vaccinations with APVAC1 (400 μg per peptide, intradermal, 11 vaccinations scheduled) started on day 15 of the first adjuvant TMZ cycle (see Extended Data Fig. 2b for schedule details). GM-CSF (75 μg, intradermal) and poly-ICLC (1.5 mg, subcutaneous) were used as immune modulators and were applied near the APVAC injection site. APVAC2 vaccines were applied starting on day 15 of the fourth adjuvant TMZ cycle (400 μg per peptide, intradermal, 8 vaccinations scheduled), usually leading to co-application of APVAC1 and APVAC2 at three visits (Fig. 1). After completion of the regular APVAC vaccinations or after progression, it was possible to continue vaccinations if this was in the patient's best interest and if medication was still available. Continued vaccinations beyond the regular schedule were performed at four-weekly intervals. Nine patients received vaccinations under this 'continued vaccination' option. Exposure to standard therapy was not altered for patients in the GAPVAC-101 trial (Extended Data Fig. 2d). Primary end points of the trial were safety and tolerability, feasibility of the personalized approach and biological activity.

APVAC1 selection and manufacturing. The fresh-frozen tumour samples of patients underwent central pathology review to enrich for necrosis-free tumour pieces with high tumour-cell contents. Tumour-cell-enriched specimens were lysed and HLA class I- and class II-associated peptides were isolated and analysed by mass spectrometry as previously described[17]. In brief, HLA-peptide extracts were separated by reversed-phase chromatography (nanoAcquity UPLC system) using ACQUITY UPLC BEH C18 columns (75 μm × 250 mm, Waters). Mass spectrometry was performed on Orbitrap LTQ Velos or Fusion mass spectrometers (ThermoFisher Scientific) by data-dependent acquisition using collision-induced dissociation as well as higher-energy collisional dissociation. Furthermore, genomic DNA and mRNA were isolated from the same lysate for mutanome and gene-expression analyses, respectively. mRNA was quality-controlled and analysed by gene microarray analysis using Affymetrix Human Genome U133 Plus 2.0 oligonucleotide microarrays (Affymetrix). Finally, PBMCs of the patient were assessed for precursor T cells that were specific for the APVAC1 peptides as previously described[30]. In brief, CD8$^+$ T cells were stimulated in vitro under limited dilution conditions (usually 12 wells per peptide) using artificial antigen-presenting cells. Wells with >1% specific CD8$^+$ T cells as per multimer staining after three weeks of culture were counted as positive. If no individual immunogenicity data were available for the patient (patient 13), the percentage of positive wells in healthy donors was used as surrogate. For each patient, a ranking score was calculated for each warehouse peptide, considering the individual peptide-presentation data, mRNA expression data and immunogenicity data (see Supplementary Methods 'APVAC1 selection process' for details). In brief, the different parameters were transformed into probability scores (values between 0 and 1) using a Bayesian method. The rank score of a warehouse peptide constitutes a probabilistic score that ensured strong tumour association as well as sufficient immunogenicity for highly ranked peptides. For each patient, the seven best-ranked peptides were selected into the personalized APVAC1 composition (as shown for patient 5 in Extended Data Fig. 1a) together with a viral marker peptide (HBV-001 or HCV-002) and BIR-002/PTP-010 as invariant pan-HLA-DR (class II)-binding peptides (PTP-010 was replaced by BCA-005 for two compositions owing to stability issues). Finally, APVAC1 compositions were reviewed and approved by a Target Selection Committee. The peptides were formulated into single-dose vials and released according to GMP at the manufacturing site of the Department of Immunology, University of Tübingen.

APVAC2 selection and manufacturing. For APVAC2, tumour-specific somatic mutations were analysed by BioNTech from the DNA and RNA samples extracted from high-quality enriched tumour materials compared to DNA from normal blood cells from the same patient using next-generation sequencing. Whole-exome sequencing libraries were prepared using Agilent's SureSelect V6 XT Kit. From the tumour RNA, poly(A)-based RNA sequencing libraries were prepared using TruSeq (Illumina). For samples with a tumour content above 40%, whole-exome and RNA sequencing libraries were prepared in singletons and sequenced paired-end for 50 nucleotides on an Illumina HiSeq 2500, aiming for a minimum of 150 million reads per library. For samples that had a tumour content below 40%, library preparation and sequencing were done in duplicates. All mutanome-related data analysis steps were coordinated by a software pipeline. For the DNA libraries, a minimum of 150×10^6 paired-end 50-nucleotide reads and for the RNA libraries a minimum of 75×10^6 paired-end 50-nucleotide reads were required. For mutation detection, DNA reads were aligned to the reference genome hg19 with BWA[31]. Exomes from tumour and matched normal samples were analysed for single-nucleotide variants. Loci with putative homozygous genotypes in the normal samples were identified and filtered to retain high-confidence calls for single-nucleotide variants. The remaining sites were further inspected for a putative homozygous or heterozygous mutational event. Suspected sites were filtered to remove potential false positives. The final list of single-nucleotide variants consisted of high-confidence homozygous sites in the normal samples and high-confidence heterozygous or homozygous mutational events in the tumour samples. Genomic coordinates of identified variants were compared with known transcript coordinates for genes of the University of California Santa Cruz (UCSC) at https://github.com/brentp/cruzdb to associate the variants with genes, transcripts, potential changes in amino acid sequences and the RNA-sequencing-derived expression values. For RNA-sequencing analyses, RNA reads were aligned to the hg19 reference genome and transcriptome using Bowtie[32], and gene expression was determined by comparison with known transcript and exon coordinates of genes of the UCSC, followed by normalization to reads per kilobase million (RPKM) units[33]. High-sensitivity liquid chromatography–tandem mass spectrometry data were analysed against a personalized proteome library that contained all single-nucleotide variants to identify HLA class I- and class II-presented, mutation-containing peptides. Mass spectrometry-confirmed mutations containing HLA epitopes would have gained priority for APVAC2 (but were not detected). As a second track, predicted variants were selected from the identified single-nucleotide variants by first removing non-sense variants and filtering by non-zero exon and transcript expression and then sorting by exon expression followed by HLA class I-binding prediction score using a stable sorting algorithm. HLA-binding affinity was predicted via the Immune Epitope Database (IEDB) T cell prediction tools (version 2.5, IEDB-recommended mode)[34] using all variant-containing 8–11 amino acid-containing peptides for HLA-A/B-binding estimations. Out of all predictions for a single variant, the best IEDB consensus score was associated with the respective variants. Potential immunogenicity was assessed by calculating the difference between the predicted HLA-binding affinity of the mutant peptide and the wild-type counterpart as well as absolute predicted HLA binding and variant expression, by analogy with a previously published algorithm[35]. A shortlist of up to 46 single-nucleotide variants was selected for confirmation by Sanger sequencing. For primer design, genomic sequences that flanked the mutation sites were extracted from the reference genome and used as input for the Primer3 software[36,37]. The output primer pairs were aligned to the reference genome using BLAT[38]. Primer pairs that aligned to off-target loci were removed, and the remaining optimal primer pair was returned for each input site. Sanger sequencing was performed by amplifying each selected mutated locus from DNA of tumour tissues and white blood cells by PCR (15 min at 95 °C for the initial activation followed by 35 cycles of 30 s at 94 °C for denaturation, 30 s at 60 °C for annealing, 30 s at 72 °C for extension, and 6 min at 72 °C for the final extension). Each PCR product was quality-controlled using a QIAxcel (Qiagen) device and

purified via ExoI/AP treatment. Sanger sequencing was performed by Eurofins/MWG. From the confirmed mutations, only the highest-ranking ones as judged by HLA binding, expression and immunogenicity were considered for APVAC2 as 19 amino acid peptides (mutation flanked by 9 amino acids of the natural sequence on each side to cover all potential mutation-containing HLA-binding 9–10 amino acid peptides, while minimizing the number of contained potential HLA binders that do not contain the mutation). As a third track, HLA class I peptidome data were assessed for tumour-associated unmutated peptides not contained in the warehouse. Highly promising candidates were integrated into the prioritized ranking (without immunogenicity pretesting). The Target Selection Committee selected the most promising candidates from all APVAC2 tracks to a ranked shortlist with up to four candidates. The final selection also considered variant allele frequency, tissue distribution of wild-type source gene expression and confirmation of mutations by Sanger sequencing. Manufacturability of the four candidates was tested under non-GMP conditions. If successful, the two highest-ranking APVAC2 peptides were de novo synthesized, formulated under GMP conditions and filled into single-use vials at the manufacturing site of the Department of Immunology, University of Tübingen. For patients 1, 2, 6, 12 and 15, low yield and/or purity of an APVAC2 peptide candidate required replacement by backup candidates or removal of one peptide (patients 6 and 12). For patient 6, first application of APVAC2 was delayed by one TMZ cycle owing to delays in manufacturing. In all other cases, GMP manufacturing of APVAC2 was completed in time.

Clinical assessments and feasibility assessment. Safety in this trial was analysed based on the occurrence of adverse events, which were categorized according to the US National Cancer Institute's Common Terminology Criteria for adverse events version 4.0 and summarized on the preferred term level of the Medical Dictionary for Regulatory Activities version 18.0 and according to their potential relation to study drugs (APVAC vaccines, GM-CSF or poly-ICLC) and TMZ treatment. Operational feasibility was assessed based on success rates and duration of APVAC1 and APVAC2 definition and manufacturing processes. Magnetic resonance imaging scans were taken according to European Society of Medical Oncology guidelines[39] and evaluated based on the criteria defined by the Neuro-Oncology Working Group[40], taking special care in the aspect of potential pseudo-progression, which may be frequent in immunotherapy trials owing to immune cell infiltration into the glioblastoma tumour[14].

Immune response assessment and biomarker analyses. At different time points pre- and post-vaccination (Fig. 1), PBMCs for immunomonitoring were isolated within 8 h of venipuncture from sodium heparin blood samples of patients by standard Ficoll–Hypaque density gradient centrifugation. Cells were cryopreserved in serum-free medium until standardized assessment of immune responses (Immatics). Thawed PBMC samples were labelled with CD8 microbeads (Milteny Biotec) and the $CD8^-$ T cell fraction was separated from $CD8^-$ cells by MultiMACS device according to the manufacturer's instructions. Both cell fractions were rested overnight.

HLA class I ex vivo 2D multimer assay. Ultraviolet exchange was used to create peptide:MHC (pMHC) monomers loaded with specific APVAC peptides as previously described[41]. An anti-β2-microglobulin enzyme-linked immunosorbent assay (ELISA) was performed to confirm the efficiency of peptide exchange. For each peptide to be tested, two pMHC multimers of the same specificity but with two different fluorochromes were combined as previously described[42]. All APVAC and control pMHC multimer solutions for a given patient were combined to one personalized pMHC multimer staining cocktail. Potential aggregates were removed by centrifugation. Staining was performed as previously described[43]. In brief, between 1.5×10^6 and 5×10^6 $CD8^+$ T cells were treated first with Life/Dead near-infrared dye (Life Technologies), followed by patient-individual 2D multimer staining[18] (each pMHC multimer at a concentration of 1–5 μg ml^{-1}) and surface staining with the following antibodies: CD8–fluorescein isothiocyanate (FITC; SK1, BioLegend), CD279/PD-1–BV786 (EH12.1, BD); CD197/CCR7–phycoerythrin (PE)–CF594 (150503, BD); CD45RA–AF700 (HI100, BioLegend) and CD4 (RPA-T4, BD), CD14 (61D3, ebioscience), CD16 (3G8, BD) and CD19 (HIB19, BD) antibodies for dump channel (all PE–Cy5). All washing steps were carried out in phosphate-buffered saline (PBS), 2% fetal calf serum (FCS), 2 mM ethylenediaminetetraacetic acid (EDTA) and 0.01% azide. Stained cells, fixed with FACS Perm2 solution (BD), were acquired on a LSRII SORP flow cytometer (BD) and analysed by FlowJo software version 10.1 (Tree Star). Two-dimensional multimer-positive cells had to be positive for the corresponding fluorochrome combination, but negative for any other fluorochrome as determined by Boolean gating[42]. The gating strategy is shown in Extended Data Fig. 10a. The presence of a vaccine-induced response was determined according to predefined criteria[43]. In brief, frequencies of 2D multimer-positive cells among $CD8^+$ T cells had to be at least twofold above the corresponding frequency before vaccination and had to form a clustered population that was discrete from multimer-negative cells. Staining against viral control antigens was performed for each donor. Influenza-derived peptide FLUM-001 (GILGFVFTL, HLA-A*02) and/or Epstein–Barr virus (EBV)-derived peptide EBV-014 (TYSAGIVQI, HLA-A*24) were used as positive controls; human immunodeficiency virus (HIV)-derived peptides HIV-001 (ILKEPVHGV, HLA-A*02) and/or HIV-015 (RYPLTFGW, HLA-A*24) were used as negative controls. Viral marker peptides (HBV-001 or HCV-002) were co-vaccinated in APVAC1 and used as vaccination controls[44,45]. For each stain experiment, two healthy donors (one HLA-A*02^+, one HLA-A*24^+) were used as external assay controls. Patient 9 and 11 were vaccinated with APVAC1 but were not evaluable, as they left the study before post-vaccination PBMCs were available. For patient 16, only one post-vaccination time point was available and was included post hoc into the APVAC1 immune response analysis. The memory cell induction factor (MCIF) for patients was calculated as follows. The sum of frequencies of all APVAC1-specific $CD8^+$ T cells of central memory ($CD45RA^-CD197^+$), effector memory ($CD45RA^-CD197^-$) and effector memory RA ($CD45RA^+CD197^-$) phenotypes was calculated per assay time point. In cases in which no event was detected, 0.1 event per antigen specificity was assumed. Next, the ratios of these memory cell frequencies post-vaccination versus pre-vaccination were calculated for each post-vaccination time point. The MCIF for a patient was defined as the maximum of these ratios. For patient 4, BCA-002- and PLEKHA4-001-reactive T cells were present before vaccination and did not expand, resulting in a low MCIF despite high frequencies (Fig. 2a).

Ex vivo HLA class II ICS assay. After overnight rest, between 1.7 and 5.1×10^6 $CD8^-$ T cells per well were incubated with antigenic peptide (10 μg ml^{-1}) in the presence of monensin and brefeldin A as per the manufacturer's instructions (both BD) for 6 h at 37 °C. Cells of each assay time point were stimulated with the corresponding APVAC1 class II peptides. Furthermore, cells were stimulated with mock peptide (solvent only) as an internal negative, and a CMV-002 (LPLKMLNIPSINVH)/CEFT peptide pool MHC class II (Panatecs) as a positive, control. Additionally, in each assay two healthy donors were used as external controls and stimulated using mock, HIV-001/HIV-015 as negative and a pool of CMV-002, EBV-014, influenza-derived FLUM-001 (GILGFVFTL) and CEFT peptides as positive controls. After stimulation, $CD8^-$ cells were treated with Life/Dead near-infrared dye (Life Technologies), followed by surface-staining using a CD8–BV570 (RPA-T8, BioLegend) antibody. After a washing step in PBS, 2% FCS, 2 mM EDTA and 0.01% azide, cells were fixed using FACS Perm2 solution (BD) and intracellular staining was carried out using PermWash (BD) and CD3–BV711 (OKT3, BioLegend), CD4–BV605 (OKT4, BioLegend), CD154–FITC (TRAP1, BD), IFNγ–PE–Cy7 (4S.B3, BD), interleukin (IL)-2–BV510 (MQ1-17H12, BioLegend), IL-4–BV421 (MP4-25D2, BioLegend), IL-5–PE (JES1-39D10, 1:10, BD), IL-10–allophycocyanin (APC) (JES3-9D7, Miltenyi) and tumour necrosis factor (TNF)–AF700 (MAb11, BD) antibodies. Cells were acquired and analysed as described above. Gating and analysis of vaccine-induced responses was performed according to recommendations of the Cancer Immunotherapy Immunoguiding Program[46] (Extended Data Fig. 10b). Out of 7 cytokines or markers, all $2^7 = 128$ possible combinatorial patterns were calculated using Boolean gating. To be defined as a vaccine-induced response, the frequency of cytokine-positive cells within one combinatorial pattern had to be at least twofold over the frequency in the corresponding mock control and the frequency before vaccination.

HLA-class I and class-II pan-ICS assay. PBMC samples were incubated with 0.5 U ml^{-1} benzonase (Merck). APVAC2- or control peptide-specific $CD4^+$ and $CD8^+$ T cells were amplified by a single round of IVS for 12 days using 2.5×10^6 PBMCs per well, 10 μg ml^{-1} of antigenic peptide and 20 U ml^{-1} IL-2 (Novartis). Samples of each assay time point of a given patient were stimulated with a pool of all patient-specific full-length APVAC2 peptides as well as separately with a viral peptide pool (containing FLUM-001, CMV-002, EBV-014 and CEFT), which served as a positive control for IVS. As interassay control, two healthy donor controls were included in each individual assay. After 12 days, cells were restimulated ($0.275–1.7 \times 10^6$ cells per well) with 10 μg ml^{-1} antigen peptide in the presence of monensin, brefeldin A and CD107a–FITC (H4A3, BD) antibody for 6 h at 37 °C. Restimulation was either performed with individual full-length APVAC2 peptides or pools of all possible peptides that were nine amino acids long and predicted HLA class I epitopes that were derived from a given parental APVAC2 peptide (if applicable). Mock peptide control and stimulation with viral peptide pool as positive control were included. Stimulated cells were surface-stained using CD8–BV605 (SK1, BioLegend) before fixation with FACS Perm2 solution (BD). Intracellular staining with antibodies CD4–BV785 (RPA-T4, BioLegend), CD154–BV421 (TRAP1, BD), IFNγ–PE–Cy7 (4S.B3, BD), IL-2–BV510 (MQ1-17H12, BioLegend), IL-5–PE (JES1-39D10, BD), IL-10–BV650 (JES3-9D7, BD), IL-17–BV570 (BL168, BioLegend), IL-21–APC (3A3-N2, BioLegend) and TNF–AF700 (MAb11, BD) was carried out in PermWash buffer (BD). Cells were acquired and analysed as described above to assess cytokine-positive cells among $CD4^+$ and $CD8^+$ T cells. Gating was performed according to recommendations of the CIP (Extended Data Fig. 10c). Using Boolean gating, 77 out of 512 combinatorial patterns were selected, reflecting the cytokine expression profiles of T_H cell subsets as previously described[47]. To be defined as a vaccine-induced response, the

frequency of cytokine-positive cells within one combinatorial pattern had to be at least fourfold over the frequency of the corresponding mock control and the frequency before vaccination.

IFNγ enzyme-linked immunospot assay. Detailed protocols have previously been described[48,49]. In brief, for Fig. 5d, PBMCs from patient 8 were thawed and expanded for 12 days in the presence of 5 μg ml^{-1} peptide and 2 ng ml^{-1} recombinant human IL-2 (R&D). Cells were collected and tested in duplicates by IFNγ enzyme-linked immunospot assay (ELISPOT) with 2.5 μg ml^{-1} peptide, 10 μg ml^{-1} phytohaemagglutinin (PHA)-L as positive control or 10% dimethyl sulfoxide (DMSO) as mock. After 26 h incubation, spots were revealed with 5-bromo-4-chloro-3-indolyl-phosphate/nitro-blue tetrazolium chloride and analysed with an ImmunoSpot Series 6 ELISPOT Reader (C.T.L. Europe).

TIL expansion protocol. A harmonized protocol for TIL expansion was established during the preclinical phase of the project. First, information on protocols established at each clinical centre for TIL isolation and in vitro expansion were compared; based on this survey, three IL-2 concentrations (150, 1,000 and 6,000 IU ml^{-1}) and the addition of a CD3 signal (soluble CD3 antibody or beads coated with CD3/CD28 antibodies) were tested for expanding glioma TILs. Cell outgrowth, cell yields and distribution of T and natural killer cell subsets were determined for 24 gliomas altogether at four centres. T cell expansion was similar in the presence of 6,000 IU ml^{-1} and 1,000 IU ml^{-1} IL-2, but lower with 150 IU ml^{-1}. CD3$^+$CD4$^+$TCRαβ$^+$ cells were prominent in most cultures, which is different when compared to what is found for melanoma (Extended Data Fig. 8a). In some individual cultures, a stronger expansion of CD8$^+$ T cells was observed (Extended Data Fig. 8c). Hence, we recommend culturing several individual cultures rather than pooling all TILs. CD3 stimulation clearly increased cell yield compared to IL-2 alone (Extended Data Fig. 8b), as previously observed[50]. In 2 out of 2 tumours tested, the CD4$^+$/CD8$^+$ T cell ratio did not change significantly over the weeks of culture (three tests at one-week intervals, data not shown). On the basis of the results obtained in these optimization experiments, a concentration of recombinant human IL-2 of 1,000 IU ml^{-1} and the addition of a CD3 antibody were finally chosen. The final GAPVAC harmonized protocol for glioblastoma TIL expansion, which was afterwards applied during the clinical phase is provided in the Supplementary Methods (see 'Harmonized GAPVAC TIL isolation and expansion protocol from glioblastoma tumour specimens').

Functional testing of TILs. TIL peptide-specificity testing was performed using ICS (for HLA class I peptides and HLA class II or long peptides) and HLA-multimer staining (for HLA class I peptides only). Both assays were harmonized during the preclinical phase by organizing successive proficiency panels ($n = 4$ in total) based on those published by the Immunoguiding programme of the Association for Cancer Immunotherapy (CIP-CIMT)[46,51,52]. For Fig. 5c, TILs were thawed, counted and allowed to rest in the presence of 1 μg ml^{-1} DNAse I. Cells were then washed and stimulated with peptides (10 μg ml^{-1}) or 10% DMSO in the presence of monensin and brefeldin A (10 μg ml^{-1}, Sigma-Aldrich). After overnight stimulation, cells were washed and stained with Zombie Aqua (Biolegend) and antibodies CD4–APC–Cy7 (BD), CD8–PE–Cy7 (Beckman Coulter) and CD3–BV711 (Biolegend) for 20 min at 4 °C, fixed and permeabilized (Cytofix/Cytoperm, BD) and stained with anti-CD154–APC, anti-IFNγ–FITC, anti-IL-2–PE (all BD) and anti-TNF–Pacific Blue (Biolegend) for 20 min at 4 °C. Cells were washed and acquired on a LSR Fortessa SORP equipped with Diva v.6.1.2 (BD). Results were analysed with FlowJo v.10. The gating strategy was: time histogram, FSC-A/FSC-H (singlets), FSC-A/Zombie Aqua (living cells), FSC-A/SSC-A (lymphocytes), FSC-A/CD3 (CD3$^+$ lymphocytes), CD4/CD8 (CD8$^-$).

Immunohistochemistry. The mouse monoclonal antibodies CD8 (clone C8/144B; DAKO) and FOXP3 (clone 236A/E7; Abcam), and the rabbit monoclonal antibody granzyme B (rb-poly; Abcam) were used in combination with Bright Vision anti-mouse antibody (Immunologic) or Bright Vision anti-rabbit antibody (Immunologic), respectively. After deparaffinization, sections were immersed into 100% ethanol (2×), 96% ethanol (2×) and 70% ethanol (2×), incubated at 120 °C for 10 min in citrate buffer (pH 6) for epitope retrieval and allowed to cool to room temperature. After quenching and blocking, the slides were incubated overnight with the first antibody followed by incubating with the second antibody for 30 min and substrate reaction using Vector NovaRED (Vector Laboratories). Cells were counterstained with Mayer's haematoxylin. Positive control slides (stomach and tonsil) without the primary antibody were included in all assays. The exact number of positive lymphocytes per mm^2 tumour tissue was evaluated after manual spot recognition by Definiens-Tissue Studio software analysis. Positive cells from four representative areas within the tumour tissue were evaluated.

TCR clonotype analysis. RNA was isolated from tumour specimens and TIL cultures using the NucleoSpin RNA kit (MACHEREY-NAGEL) according to the manufacturer's instructions. RNA was reverse-transcribed to complementary DNA (cDNA) using the SuperScript VILO cDNA Synthesis Kit (ThermoFisher Scientific). TCR clonotype mapping was carried out as previously described[53]. In brief, cDNA was amplified by PCR using a primer panel that amplified the 24 β-chain variable (BV) region families of the TCR in DNA fragments suitable for TCR clonotype mapping by electrophoresis on a denaturing gradient gel that contained 6% polyacrylamide and a gradient of urea (Sigma Life Science, Sigma-Aldrich) and formamide (Sigma-Aldrich) from 20% to 80%. Gels were run at 160–175 V for 4.5 h in TAE (0.04 M Tris-acetate and 0.001 M EDTA) and kept constantly at 56 °C. Gels were stained with cyber green and visualized under ultraviolet light.

TCR identification and in vitro expansion. APVAC1-specific T cells were sorted from post-vaccination PBMCs of patient 16. TCR sequences were obtained by single-cell rapid amplification of cDNA-end (RACE) PCR and subsequent sequencing of the α and β chains[54]. In parallel, sorted T cells were stimulated in vitro for three weeks using PHA (2 μg ml^{-1}), IL-2 (300 IU ml^{-1}), IL-7 (10 ng ml^{-1}) and IL-21 (10 ng ml^{-1}) and were subsequently used in Vital-FR killing assays.

TCR cloning. The VDJ regions of the TCR were combined in silico with mouse constant regions modified to include an additional disulfide bond, as previously described[55]. The α and β human/mouse chimeric TCR chains were codon-optimized in silico and linked by a furin cleavage site and P2A sequence to form a polycistronic transcript. Constructs were synthesized by ThermoFisher Scientific or Eurofins Genomics, before being cloned downstream of an *EF1A* (also known as *EEF1A1*) promoter in a mammalian transient expression vector using golden gate assembly.

Cloning of overexpression constructs. cDNA of *NLGN4X* in a pDONR vector was provided by R. Will of the DKFZ GPCF Vector and Clone Repository. An internal ribosomal entry site (IRES) sequence was appended to the NanoLuc luciferase sequence using tailed primer PCR, and the resulting PCR product was inserted into pDONR P2rP3 using Gateway BP cloning. The phosphoglycerate kinase 1 (*PGK1*) promoter was inserted into pDONR P4-P1r using tailed primer PCR and Gateway BP cloning. Expression vectors that combined the *PGK1* promoter, the full-length cDNA of *NLGN4X* or *NRCAM*, and the IRES-NanoLuc luciferase marker were assembled using Multisite Gateway LR cloning.

Electroporation of T cells and transfection of target cells. T cells were isolated from PBMCs from HLA-A2*01$^+$ healthy donors using the MagniSort Human T cell Enrichment Kit according to the manufacturer's instructions. T cells were kept in TexMACS without phenol red and activated with 155 U ml^{-1} human IL-7, 290 U ml^{-1} human IL-15 and T Cell TransAct. Vector DNA was prepared using a ZymoPURE II plasmid maxiprep kit (Zymo Research). Plasmid DNA was electroporated using a Neon electroporator (ThermoFisher Scientific; pulse voltage 2,200 V, pulse width 20 ms, pulse number = 1, cell density = 5 × 10^6). Transfection of HLA-A*02:01$^+$ U87MG cells was done using FuGENE HD (Promega).

Cytotoxicity assays. Avidity of APVAC1-specific T cells as shown in Fig. 2c was analysed using the Vital-FR assay[56]. In brief, T cells were co-cultured with carboxyfluorescein succinimidyl ester (CFSE)-labelled K562-A2 cells loaded with titrated amounts of test peptide and FarRed-labelled K562-A2 cells loaded with an irrelevant peptide. After 20 h, numbers of CFSE- and FarRed-labelled cells were assessed by flow cytometry and specific lysis was calculated. For peptide titration experiments (Extended Data Fig. 3d), T2 cells were stained with Vybrant DiD and T cell clones with CFSE. Co-culture (4 h) was performed with increasing concentrations of peptide (effector-to-target ratio (*E:T*) = 10:1). Cell death was measured by addition of 7-aminoactinomycin D (7AAD) and detection of 7AAD$^+$ Vybrant DiD$^+$ T2 cells by flow cytometry. For NanoLuc luciferase-based killing assays, TCR-engineered T cells and transfected U87MG target cells (*NLGN4X* and *NRCAM*) were co-cultured for 9 h. Supernatants were carefully removed to remove cell debris. After addition of new medium, the Nano-Glo Luciferase Assay System (Promega) was used according to the manufacturer's instructions to measure NanoLuc luciferase expression. For LDH-based killing assays, autologous (NLGN4X-001-reactive, PTP-013-reactive) and HLA-A*02:01$^+$ T cells were rested overnight and co-cultured for 9 h with HLA-A2*01$^+$ glioma-initiating cell lines (L2 or P3XX). A CytoTox96 Non-Radioactive Cytotoxicity Assay (Promega) was used according to the manufacturer's instructions to quantify LDH release. Absorbance was measured at 490 nm. Cell lines are tested monthly for the absence of mycoplasma. Cell line authentication is ensured by genetic testing using Gene Print (Promega). L2 and P3XX are primary cells immediately derived from human tumours (provided by H. Miletic, K. G. Jebsen Brain Tumour Research Centre, University of Bergen).

Assessment of T_{reg} cell frequencies. Cryopreserved PBMC samples were thawed and 1.5 × 10^6 PBMCs were stained with the following antibodies: CD3–Pacific Blue (clone SK7, Biolegend), CD4–APC–Cy7 (clone SK3, Biolegend), CD25–APC (clone M-A251, Biolegend), CD45RA–PerCP–Cy5.5 (clone HI100, Biolegend), CD127–PE–Cy7 (clone HIL-7R-M21, BD), FOXP3–AF488 (clone 259D/C7, BD), KI-67–PE (clone Ki67, Biolegend) and the Live/Dead marker Zombie Aqua (Biolegend). Cell-surface antibody staining was performed in PBS, 0.5% BSA and 0.01% azide for 30 min at 4 °C. Intranuclear staining was conducted with the True-Nuclear Transcription Factor Buffer set (Biolegend) according to the manufacturer's instructions; antibody staining was for 40 min at 4 °C. Stained cells were acquired on a BD FACSCanto II and analysed using FlowJo software v.10.4.

At least 500,000 events were acquired per sample. Gating and enumeration of T_{reg} cells was based on CD25, CD127 and FOXP3 expression (Extended Data Fig. 10d), as previously described[57].

Statistical analyses. Clinical data collection and management was carried out using SAS (v.9.3; SAS Institute). Where applicable, data were reported as the median (indicating the range from minimum to maximum value occurred) and arithmetic mean ± s.d., as specified (R software package v.3.4.1). Dichotomous variables were evaluated by Fisher's exact test, whereas continuous variables were compared by two-sided Student's *t*-test or Mann–Whitney *U*-test, as indicated. Overall and progression-free survival (both calculated from primary tumour diagnosis) were assessed by Kaplan–Meier analysis using Prism 7 (GraphPad Software). An independent data safety monitoring board oversaw the study. Patient PBMCs were limited in this study. If not stated otherwise, and owing to limited sample availability, immune response assessments could only be performed once and were not repeated. As detailed in the sections for ex vivo 2D multimer, ex vivo ICS and pan-ICS analyses, various internal and external controls were included and per assay type, all patient assays were done with the same batches of critical reagents (for example, staining antibodies). Furthermore, all patient assays were performed according to detailed standard operating procedures.

Reporting summary. Further information on research design is available in the Nature Research Reporting Summary linked to this paper.

Data availability

Raw data that support the findings of this study shown in Figs. 2–4 and Extended Data Figs. 1, 3–8 and 10 are available from the corresponding author upon reasonable request. Data in Fig. 5, Extended Data Fig. 9, Table 1 and Supplementary Table 5 are on patient outcomes from the clinical study. These data will be available upon reasonable request to the corresponding author from the GAPVAC-101 study case record forms. Supplementary Tables 1–4 represent raw data and should be used to recapitulate the findings demonstrated in this study. Mass spectrometry data for sequence identification of APVAC warehouse peptides have been deposited at the PeptideAtlas (http://www.peptideatlas.org/) with the dataset identifier PASS01284. mRNA microarray data used for APVAC selection are available at Gene Expression Omnibus (GSE122498). All mutations found in the DNA sequencing are depicted in the manuscript. The uploading of DNA sequencing data with the potential for patient identification was not included in the informed consent that patients gave to the trial; these data will be shared (with identifying information removed) upon reasonable request.

28. Singh-Jasuja, H., Emmerich, N. P. & Rammensee, H. G. The Tübingen approach: identification, selection, and validation of tumor-associated HLA peptides for cancer therapy. *Cancer Immunol. Immunother.* **53**, 187–195 (2004).
29. Stupp, R. et al. Radiotherapy plus concomitant and adjuvant temozolomide for glioblastoma. *N. Engl. J. Med.* **352**, 987–996 (2005).
30. Walter, S. et al. Cutting edge: predetermined avidity of human CD8 T cells expanded on calibrated MHC/anti-CD28-coated microspheres. *J. Immunol.* **171**, 4974–4978 (2003).
31. Li, H. & Durbin, R. Fast and accurate short read alignment with Burrows–Wheeler transform. *Bioinformatics* **25**, 1754–1760 (2009).
32. Langmead, B., Trapnell, C., Pop, M. & Salzberg, S. L. Ultrafast and memory-efficient alignment of short DNA sequences to the human genome. *Genome Biol.* **10**, R25 (2009).
33. Mortazavi, A., Williams, B. A., McCue, K., Schaeffer, L. & Wold, B. Mapping and quantifying mammalian transcriptomes by RNA-seq. *Nat. Methods* **5**, 621–628 (2008).
34. Kim, Y. et al. Immune epitope database analysis resource. *Nucleic Acids Res.* **40**, W525–W530 (2012).
35. Kreiter, S. et al. Mutant MHC class II epitopes drive therapeutic immune responses to cancer. *Nature* **520**, 692–696 (2015).
36. Koressaar, T. & Remm, M. Enhancements and modifications of primer design program Primer3. *Bioinformatics* **23**, 1289–1291 (2007).
37. Untergasser, A. et al. Primer3—new capabilities and interfaces. *Nucleic Acids Res.* **40**, e115 (2012).
38. Kent, W. J. BLAT—the BLAST-like alignment tool. *Genome Res.* **12**, 656–664 (2002).
39. Stupp, R., Brada, M., van den Bent, M. J., Tonn, J. C. & Pentheroudakis, G. High-grade glioma: ESMO Clinical Practice Guidelines for diagnosis, treatment and follow-up. *Ann. Oncol.* **25**, iii93–iii101 (2014).
40. Wen, P. Y. et al. Updated response assessment criteria for high-grade gliomas: response assessment in neuro-oncology working group. *J. Clin. Oncol.* **28**, 1963–1972 (2010).
41. Rodenko, B. et al. Generation of peptide-MHC class I complexes through UV-mediated ligand exchange. *Nat. Protoc.* **1**, 1120–1132 (2006).
42. Hadrup, S. R. et al. Parallel detection of antigen-specific T-cell responses by multidimensional encoding of MHC multimers. *Nat. Methods* **6**, 520–526 (2009).
43. Walter, S. et al. Multipeptide immune response to cancer vaccine IMA901 after single-dose cyclophosphamide associates with longer patient survival. *Nat. Med.* **18**, 1254–1261 (2012).
44. Bertoletti, A. et al. Definition of a minimal optimal cytotoxic T-cell epitope within the hepatitis B virus nucleocapsid protein. *J. Virol.* **67**, 2376–2380 (1993).
45. Livingston, B. D. et al. The hepatitis B virus-specific CTL responses induced in humans by lipopeptide vaccination are comparable to those elicited by acute viral infection. *J. Immunol.* **159**, 1383–1392 (1997).
46. Welters, M. J. et al. Harmonization of the intracellular cytokine staining assay. *Cancer Immunol. Immunother.* **61**, 967–978 (2012).
47. Zhu, J., Yamane, H. & Paul, W. E. Differentiation of effector CD4 T cell populations. *Annu. Rev. Immunol.* **28**, 445–489 (2010).
48. Loffler, M. W. et al. Personalized peptide vaccine induced immune response associated with long-term survival of a metastatic cholangiocarcinoma patient. *J. Hepatol.* **65**, 849–855 (2016).
49. Widenmeyer, M. et al. Promiscuous survivin peptide induces robust $CD4^-$ T-cell responses in the majority of vaccinated cancer patients. *Int. J. Cancer* **131**, 140–149 (2012).
50. Grimm, E. A. et al. Characterization of interleukin-2-initiated versus OKT3-initiated human tumor-infiltrating lymphocytes from glioblastoma multiforme: growth characteristics, cytolytic activity, and cell phenotype. *Cancer Immunol. Immunother.* **32**, 391–399 (1991).
51. Britten, C. M. et al. The CIMT-monitoring panel: a two-step approach to harmonize the enumeration of antigen-specific $CD8^-$ T lymphocytes by structural and functional assays. *Cancer Immunol. Immunother.* **57**, 289–302 (2008).
52. van der Burg, S. H. et al. Harmonization of immune biomarker assays for clinical studies. *Sci. Transl. Med.* **3**, 108ps44 (2011).
53. Thor Straten, P. et al. In situ T cell responses against melanoma comprise high numbers of locally expanded T cell clonotypes. *J. Immunol.* **163**, 443–447 (1999).
54. Kobayashi, E. et al. A new cloning and expression system yields and validates TCRs from blood lymphocytes of patients with cancer within 10 days. *Nat. Med.* **19**, 1542–1546 (2013).
55. Cohen, C. J. et al. Enhanced antitumor activity of T cells engineered to express T-cell receptors with a second disulfide bond. *Cancer Res.* **67**, 3898–3903 (2007).
56. Stanke, J. et al. A flow cytometry-based assay to assess minute frequencies of $CD8^+$ T cells by their cytolytic function. *J. Immunol. Methods* **360**, 56–65 (2010).
57. Santegoets, S. J. et al. Monitoring regulatory T cells in clinical samples: consensus on an essential marker set and gating strategy for regulatory T cell analysis by flow cytometry. *Cancer Immunol. Immunother.* **64**, 1271–1286 (2015).

a

Peptide Code	Rank Score	Selected	Immuno-genicity	Tumor association: Peptide Presentation: Detected by MS	Tumor association: Peptide Presentation: Exclusive on tumors	Tumor association: Peptide Presentation: Overpresentation ratio	mRNA over-expression ratio
BCA-002	0.993	+	100%	+	+	48.4	10.6
CDK4-001	0.967	+	100%	+	-	74.6	1.3
PTP-013	0.963	+	58%	+	+	1243.3	51.1
PTP-005	0.955	+	50%	+	+	265.8	51.1
CSRP2-001	0.942	+	42%	+	-	230.6	2.6
ELOVL2-001	0.931	+	33%	+	-	32.1	4.6
RAD54B-001	0.896	+	58%	+	+	13.6	1.6
MTSS1L-001	0.891	-	75%	+	-	481.4	n.d.
VPS13B-001	0.889	-	83%	+	-	8.1	1.9
USP11-001	0.886	-	33%	+	+	25.9	n.d.
PCDHGC5-001	0.880	-	42%	+	-	1217.2	n.d.
DPYSL4-001	0.869	-	17%	+	-	100.0	4.8
NLGN4X-001	0.867	-	17%	+	+	42.6	10.5
CLU-001	0.859	-	17%	+	-	291.2	1.5
GRIK3-001	0.801	-	17%	+	+	278.1	n.d.
DCA-001	0.799	-	8%	+	-	266.1	14.8
PLEKHA4-001	0.799	-	8%	+	-	395.9	11.3
MAGI2-001	0.789	-	8%	+	+	104.2	2.8
EIF4E-001	0.781	-	8%	+	-	89.9	1.6
PCNXL3-001	0.639	-	8%	+	-	9.6	n.d.
BCA-003	0.555	-	33%	-	+	-	10.6
NRCAM-001	0.549	-	50%	-	+	-	3.1
CERS1-001	0.381	-	0%	+	-	1230.4	n.d.
PTP-012	0.331	-	0%	+	-	96.9	51.1
GRI-002	0.331	-	0%	+	-	1155.0	4.9
TACC3-001	0.267	-	0%	+	-	25.5	1.1
SEZ6L-001	0.149	-	0%	+	+	141.2	53.3
KCN-002	0.148	-	0%	+	+	152.2	3.8
PTP-003	0.124	-	0%	+	-	898.4	51.1
MAGEF1-001	0.113	-	0%	+	-	97.8	2.2
ANKRD40-001	0.000	-	17%	-	-	-	0.5
NLGN4Y-001	0.000	-	17%	-	-	-	0.3
ORMDL1-002	0.000	-	33%	-	-	-	n.d.

b

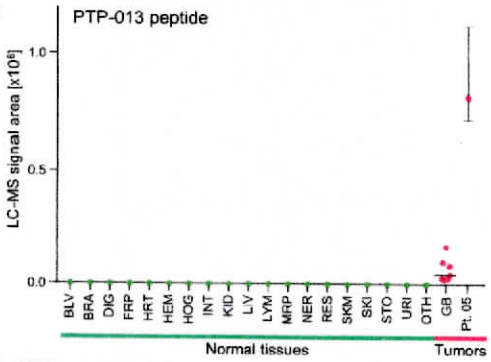

c

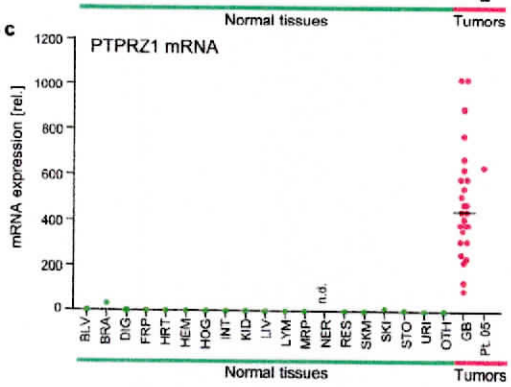

d

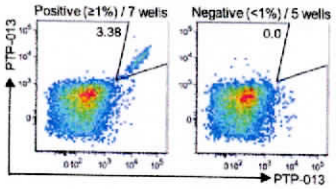

e

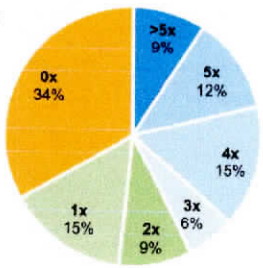

f

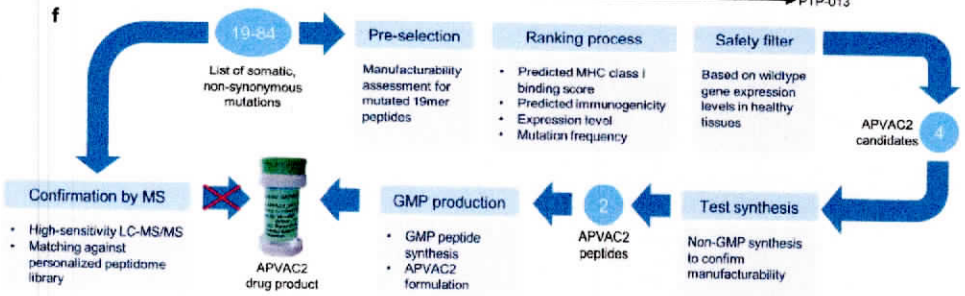

g

Rank	Selected	Gene	Mutation	Predicted MHC I score	Predicted immunogenicity	Expression / mutation frequency	Sequence
1	+	NOL12	R183W	0.2	high	high / high	KKVKEKHPRWAQDSKKPPR
2	+	COBL	V159M	0.45	medium	high / high	VPEKSVRLVMNYLRTQKAV
3	-	PTEN	L152R	0.7	medium	high / high	GKFLKAQEARDFYGEVRTR
4	-	KIAA1429	V1519G	1.55	high	high / high	NLFNNRTAYGLADVMDQL

h

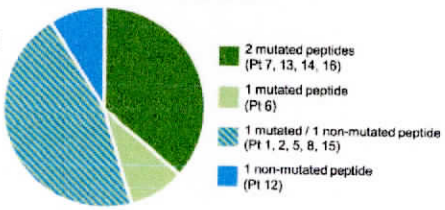

Extended Data Fig. 1 | See next page for caption.

Extended Data Fig. 1 | APVAC1 and APVAC2 processes lead to truly personalized vaccine formulations. a, Summary of biomarker data used to define APVAC1 for patient 5. Immunogenicity was calculated as the percentage of peptide-reactive wells ($n = 12$) with patient-derived PBMCs. Presentation of peptides on the tumour of patient 5 is shown as detected by mass spectrometry (present or absent). Exclusivity indicates the presence or absence of peptides in normal tissue samples ($n = 394$). Individual overpresentation ratio at the level of the HLA peptidome on comparing the tumour of patient 5 and the average of normal tissues or the limit of detection for the respective peptide (if it was never found in normal tissues). The mRNA overexpression ratio of the source genes in the tumour of patient 5 compared to the average of normal tissues. n.d., no data; genes not covered by the microarray that was used. Data were integrated into a rank score as basis for selection into APVAC1 (see Methods for details). **b**, Peptide presentation of PTP-013 on normal tissues ($n = 394$, not detected), glioblastoma specimens (identified on 7 out of 33 independent samples, median indicated), and the tumour of patient 5 as analysed by mass spectrometry. For patient 5, mean signal and signal range of $n = 5$ replicate mass spectrometry runs are shown. **c**, mRNA expression of *PTPRZ1*—which encodes PTP-013—analysed by mRNA microarray analysis in samples of pooled normal tissue mRNA, glioblastoma tumours ($n = 26$, median indicated) and tumour of patient 5. n.d., no data. **b**, **c**, BLV, blood vessels; BRA, brain; DIG, digestive glands; FRP, female reproductive organs; HRT, heart; HEM, haematopoietic cells; HOG, hormonal glands; INT, intestine; KID, kidney; LIV, liver; LYM, lymphatic tissue; MRP, male reproductive organs; NER, nervous system; RES, respiratory; SKM, skeletal muscle; SKI, skin; STO, stomach/oesophagus; URI, urinary system; OTH, other. **d**, Immunogenicity pretesting data for PTP-013 in pretreatment PBMCs of patient 5. Cells (1×10^6 per well, $n = 12$ wells tested) were stimulated with each A*02 warehouse peptide separately. After in vitro stimulation, wells were analysed for peptide-specific $CD8^+$ T cells using 2D multimer staining. Representative positive (7 out of 12) and negative (5 out of 12) wells are shown. **e**, Number of selections into APVAC1 compositions for the 33 A*02 warehouse peptides ($n = 16$ patients). **f**, APVAC2 selection process for mutated neoepitopes. **g**, The four APVAC2 candidates entering test synthesis for patient 11 are shown (patient dropped out before being vaccinated with APVAC2). Best predicted HLA class I epitopes are underlined. Red, mutated position. **h**, APVAC2 composition overview for GAPVAC-101 patients vaccinated with APVAC2 ($n = 11$).

a

	APVAC1 (warehouse selected)	APVAC2 (*de novo* manufactured)
Composition	• 7 non-mutated HLA class I peptides; individually selected and formulated from a pre-manufactured warehouse of GBM-associated peptides • 1 HLA class I viral marker peptide • 2 pan-DR binding HLA class II-restricted tumor-associated peptides	2 peptides defined via one of the following tracks: I. mutation-containing, natural presentation shown by MS (HLA class I or class II) II. mutation-containing, predicted HLA presentation and immunogenicity (19mers) III. non-mutated HLA class I peptides (presentation shown by MS, not part of warehouse)
Vaccinations (regular schedule)	11 x within 21 wks. starting day 15 of 1st TMZ cycle	8 x within 9 wks. starting day 15 of 4th TMZ cycle

b

Day	1	2	4	8	15	22	36	every 4 wks.
APVAC (400 µg i.d.)	●	●	●	●	●	●	●	●
GM-CSF (75 µg i.d.)	●	●	●	●	●	●	-	-
Poly-ICLC (1.5 mg s.c.)	●	-	●	●	●	●	●	●

c

Study drug	Number of patients exposed	Median number of applications [range]
APVAC1	15	12 [4-16]
APVAC2	11	10 [1-16]
Poly-ICLC	15	15 [3-22]
GM-CSF	15	12 [4-12]

d

ITT population (n = 16)	Mean ± SD	Median [range]	Reference median [range][28]
Time from surgery to chemoradiotherapy [days]	35.1 ± 5.7	34.5 [28-46]	35 [12-75]
Chemoradiotherapy (CRT) duration [days]	43.3 ± 1.2	43.0 [40-45]	42 [4-72]
CRT: total radiation dose [Gy]	58.8 ± 4.8	60.0 [40-60]	60 [12-72]
CRT: total TMZ dose administered [mg]	5343 ± 1136	5565 [3150-6880]	5500-6400*
Time from CRT to start of adjuvant TMZ cycles [days]	35.5 ± 6.4	34.0 [27-53]	28**
Number of adjuvant TMZ cycles	4.1 ± 1.9	5.0 [1-6]	3 [0-7]

e

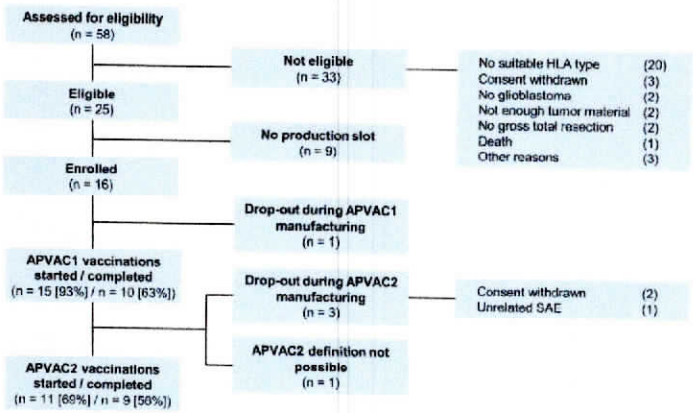

Extended Data Fig. 2 | APVAC composition, vaccination schedule, exposure to drug and standard therapy, and course of patients. **a**, Composition of personalized APVAC1 and APVAC2 drug products. **b**, Vaccination schedule for APVAC1 and APVAC2 and the immunomodulators. Note that APVAC1 and APVAC2 vaccinations started independently on day 15 of the first and fourth adjuvant TMZ cycle, respectively. In the default schedule, both APVACs were co-applied at the ninth APVAC1 and fourth APVAC2 vaccination, and at all four-weekly applications following the tenth APVAC1 and seventh APVAC2 vaccination. In case of delayed or failed APVAC production, alternative schedules were in place to optimally align vaccinations with standard therapy (data not shown). Any assessments at a vaccination visit, including blood draws for PBMC isolation, were performed prior to vaccinations. **c**, Patient exposure to study drugs. **d**, Exposure to standard therapy. Statistics on number of applications, dose and time lines between therapy phases are provided for all enrolled GAPVAC-101 patients ($n = 16$). SD, standard deviation. Reference values for the standard therapy are provided[29]. *Completed treatment assumed with 75 mg m^{-2} for 6–7 weeks calculated with 1.75-m^2 body surface area. **According to treatment schedule, patient data not published[29]. **e**, CONSORT-like diagram for patients in the GAPVAC-101 trial. Completion for APVAC1 and APVAC2 vaccinations according to the trial protocol equals to at least 11 and 8 vaccinations, respectively. Three patients left the study before receiving APVAC2: two patients withdrew their consents; one patient experienced a grade 3 seizure (unrelated to vaccinations) and withdrew from the study. Additionally, no biomarker data for definition of APVAC2 was available for patient 4, because the tumour specimen was necrotic.

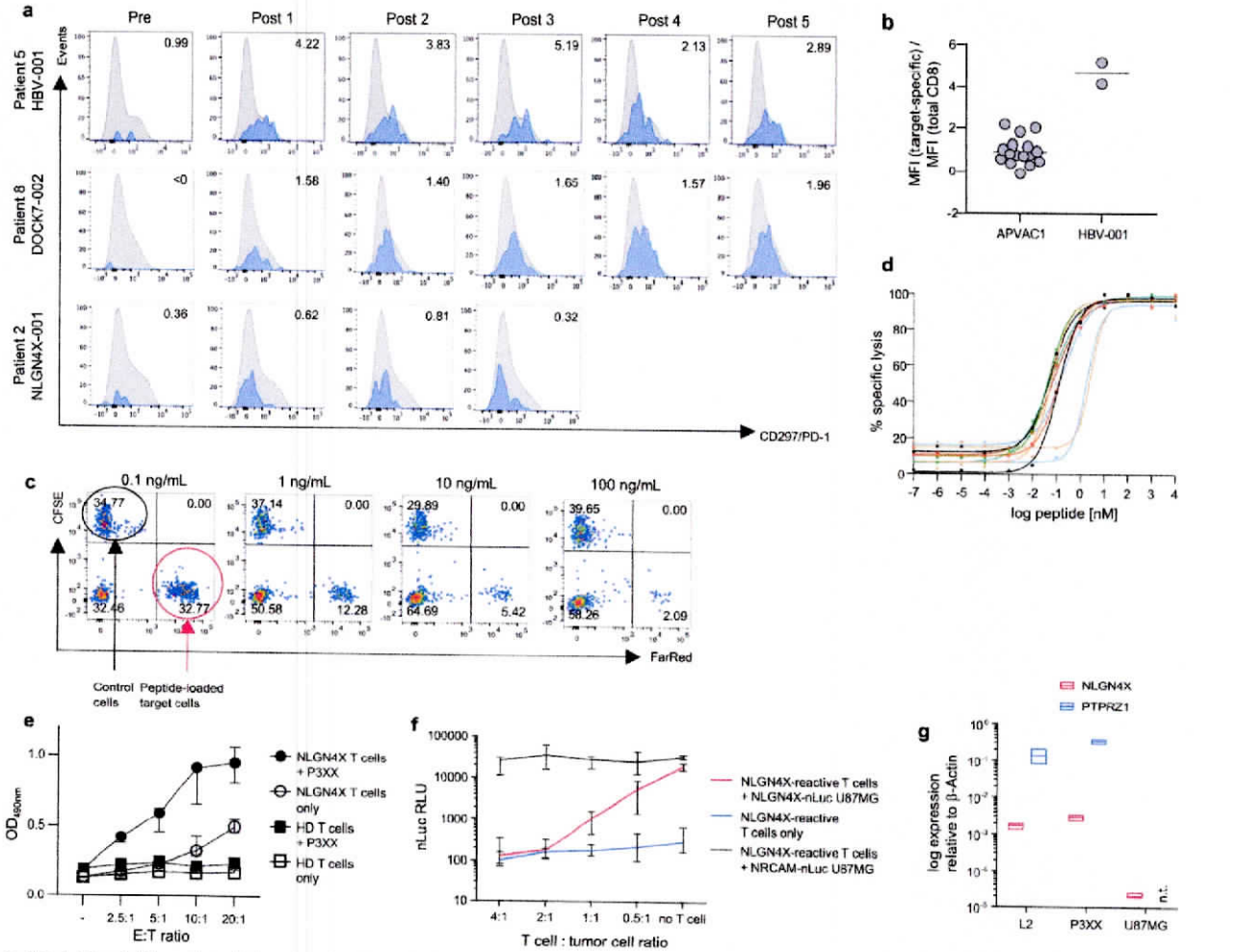

Extended Data Fig. 3 | Functional characterization of APVAC responses. a, Expression of activation/exhaustion marker PD-1 for three different immune responses pre-vaccination and at different post-vaccination time points. Top, example response to viral marker peptide HBV-001. Middle and bottom, example APVAC1-specific $CD8^+$ T cell responses. Numbers in plots show ratio of PD-1 mean fluorescence intensity (MFI) for target-specific cells (blue curve) divided by MFI of total $CD8^+$ T cells (grey curve). **b**, Summary of PD-1 evaluations as shown in **a**. Maximum MFI ratio for each $CD8^+$ T cell response to APVAC1 peptides ($n = 16$) and to the viral marker peptide HBV-001 ($n = 2$) from four patients (2, 5, 8 and 14). Data are mean and individual values. **c**, Flow cytometry data for Vital-FR assay shown in Fig. 2c. PTP-013-specific $CD8^+$ T cells were sorted from post-vaccination T cells from patient 16, in vitro-expanded for three weeks and tested for killing of CFSE-labelled K562-A2 cells loaded with titrated amounts of PTP-013 peptide in comparison to FarRed-labelled K562-A2 cells loaded with an irrelevant peptide. Data at the four lowest peptide concentrations are shown. Owing to limited availability of patient PBMCs, this experiment was performed only once with $n = 3$ replicates. **d**, BCA-002-reactive T cells from pre-vaccination PBMCs from patient 11 were cloned and expanded with PHA and IL-2. Obtained clones were tested in a flow-cytometry-based cytotoxicity assay using T2 cells loaded with titrated amounts of peptide. Results for $n = 10$ different clones are shown with calculated EC_{50} values between 49 pM and 2.8 nM (means of 2–3 replicates per clone). **e**, NLGN4X T cells as described for Fig. 2e were able to specifically lyse the $A*02^+$ glioblastoma cell line P3XX that endogenously expresses *NLGN4X* (LDH release assay). HD T cells, healthy donor-derived T cells that are not target-specific. Results from $n = 3$ replicates are shown (median and range). **f**, NLGN4X T cells were either co-cultured with the glioblastoma cell line U87MG transduced with NLGN4X–nLuc (red), irrelevant control NRCAM–nLuc (black) or in the absence of target cells (blue). With increasing *E:T* ratio, complete eradication of NLGN4X–nLuc-expressing target cells is shown (NanoLuc luciferase-based killing assays, median and range from $n = 4$ replicates shown). RLU, relative luminometer units. Additional functional data of warehouse peptides has previously been published[18]. **g**, Expression of the source genes *PTPRZ1* and *NLGN4X* in the used glioblastoma cell lines compared to the housekeeping gene *ACTB* (which encodes β-actin) measured by quantitative PCR. Boxes describe range and median from $n = 4$–6 replicates.

a

Patient	APVAC1-induced CD8⁺ T cell responses: Number of responses	Memory cells [% of total CD8⁺]	MCIF	T_{reg} pre-vaccination [% of CD4⁺]	Predominant phenotype of CD4⁺ T cell responses: APVAC1	APVAC2	APVAC2-induced CD8⁺ T cell response
16	5	0.013%	116.6	2.8	no response	T_H1	no
8	5	0.024%	59.6	3.9	T_H1	T_H1	yes
1	4	0.006%	19.1	2.1	T_H1	T_H1	no
13	7	0.017%	15.7	n.t.	no response	T_H2	yes
2	3	0.008%	12.7	2.6	T_H1	T_H1	no
7	3	0.013%	7.1	3.3	T_H1	T_H1	yes
14	5	0.007%	6.6	1.5	no response	T_H2	yes
10	5	0.013%	4.1	3.9	no response	n.e.	n.e.
5	3	0.020%	2.0	4.3	T_H1	no response	no
12	1	0.005%	1.9	6.9	T_H2	no response	no
4	3	0.066%	1.5	3.8	T_H2	n.e.	n.e.
15	1	0.005%	0.8	4.2	T_H2	T_H1	yes
6	0	0.001%	0.7	3.1	suppressive	n.e.	n.e.
Median	**3**	**0.013%**	**6.6**	**3.6**			

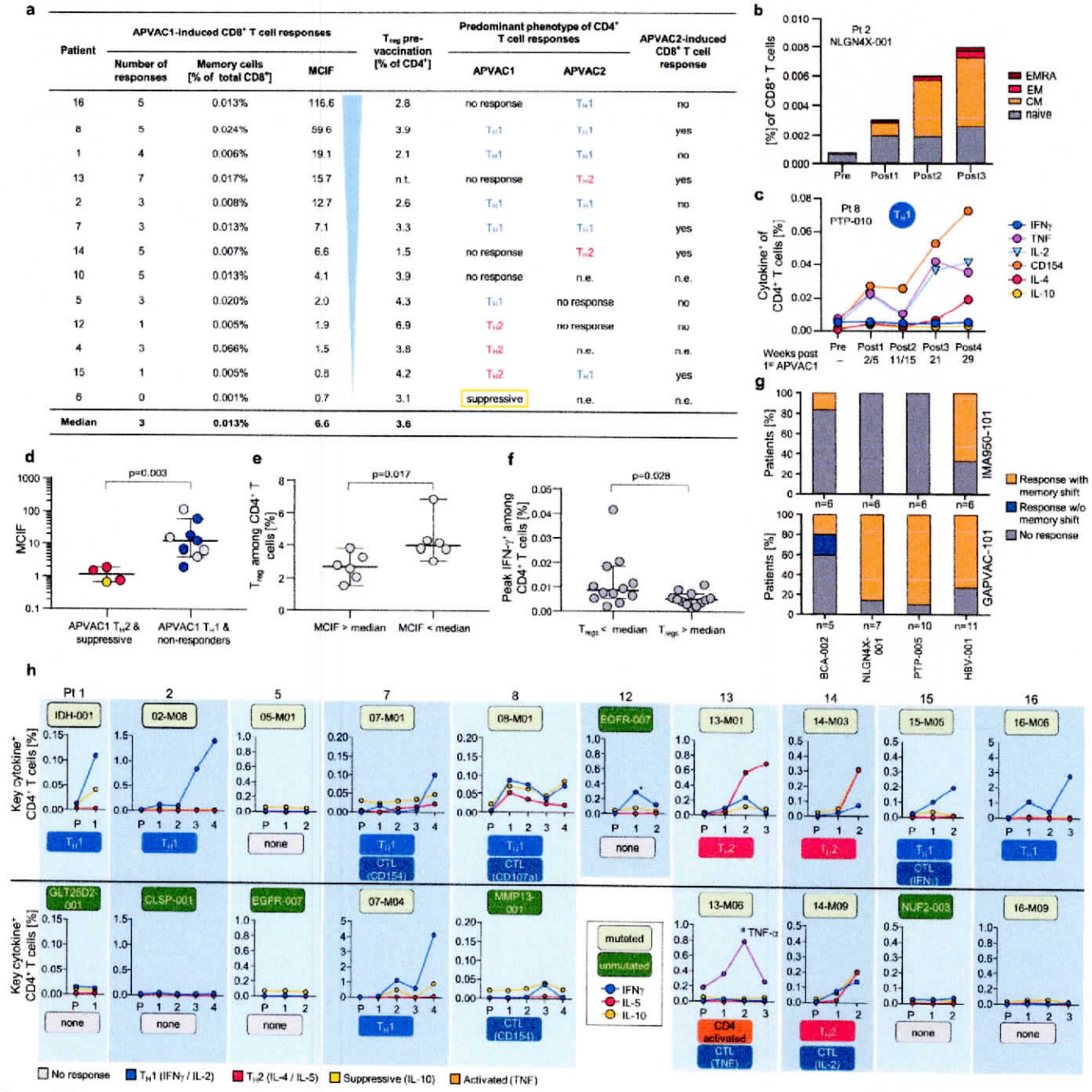

Extended Data Fig. 4 | See next page for caption.

Extended Data Fig. 4 | Additional immune response data. a, APVAC1 $CD8^+$ T cell response parameters including MCIF (see Methods), frequencies of T_{reg} cells at baseline and predominant phenotypes of APVAC-induced $CD4^+$ T cell responses for APVAC1 immune-evaluable patients ($n = 13$). n.e., not evaluable. **b**, Frequency of NLGN4X-001-specific T cells of patient 2 by differentiation phenotype summarized from the flow cytometry data shown in Fig. 2b. **c**, T_H1 $CD4^+$ T cell response against the APVAC1 HLA class II peptide PTP-010 in PBMCs from patient 8, confirming ELISPOT results (Fig. 5d) and reactivity in TILs (Fig. 5c). **d**, MCIF for GAPVAC-101 patients (evaluable for $n = 13$ patients) by APVAC1-specific $CD4^+$ T cell response type. For response type colour codes, see **a**. **e**, Pretreatment T_{reg} cells of patients with high or low MCIF (evaluable for $n = 12$ patients). **f**, Peak frequencies of IFN-γ-producing APVAC1 pan-DR peptide-specific $CD4^+$ T cells in patients with high frequencies of T_{reg} cells (>median: 3.6%) versus those with low frequencies of T_{reg} cells. Each dot represents one response ($n = 24$, two for each of the 12 evaluable patients). **d**–**f**, Median and 95% confidence interval of the median are depicted, *P* values determined by two-sided Mann–Whitney *U*-test. **g**, Immune responder rates (with and without memory shift) in GAPVAC-101 and a previous vaccine trial (IMA950-101) with the invariant multi-peptide vaccine IMA950[16] to the warehouse antigens BCA-002, NLGN4X-001, PTP-005 and the viral marker HBV-001 shared by both vaccines. Antigen responses were evaluated in both cases by the same ex vivo multimer 2D assay. Numbers below bars indicate the number of patients analysed for the respective antigen. In IMA950-101 with a comparable population of patients with glioblastoma, specific $CD8^+$ T cell responses were rarely detected ex vivo. In the GAPVAC-101 trial, measurable and sustained $CD8^+$ memory T cell responses (with at least duplication of memory cell frequencies) against the same tumour antigens were frequent. The pre-immunogenicity testing in GAPVAC-101 is probably not the main cause of the observed higher response rate, as progenitor T cells for the three compared antigens are abundant in $A*02^+$ individuals (see Supplementary Table 1). **h**, APVAC2-specific $CD4^+$ T cell responses for all evaluable patients ($n = 10$). Cell frequencies are only shown for key cytokine-positive T cells. P, prior to APVAC2 vaccination; 1–4, post-treatment measurements. Phenotype assignments as indicated. Additional $CD8^+$ T cell responses to APVAC2 peptides are indicated with the detected lead cytokine. *Pre-defined response criteria not met. #Response to 13-M06 was negative for any key cytokine. TNF^+ cells are shown. **a**–**h**, Owing to limited availability of patient PBMCs, immune response analyses were only performed once per patient. For assays with limited patient materials, see 'Statistical analyses' in Methods.

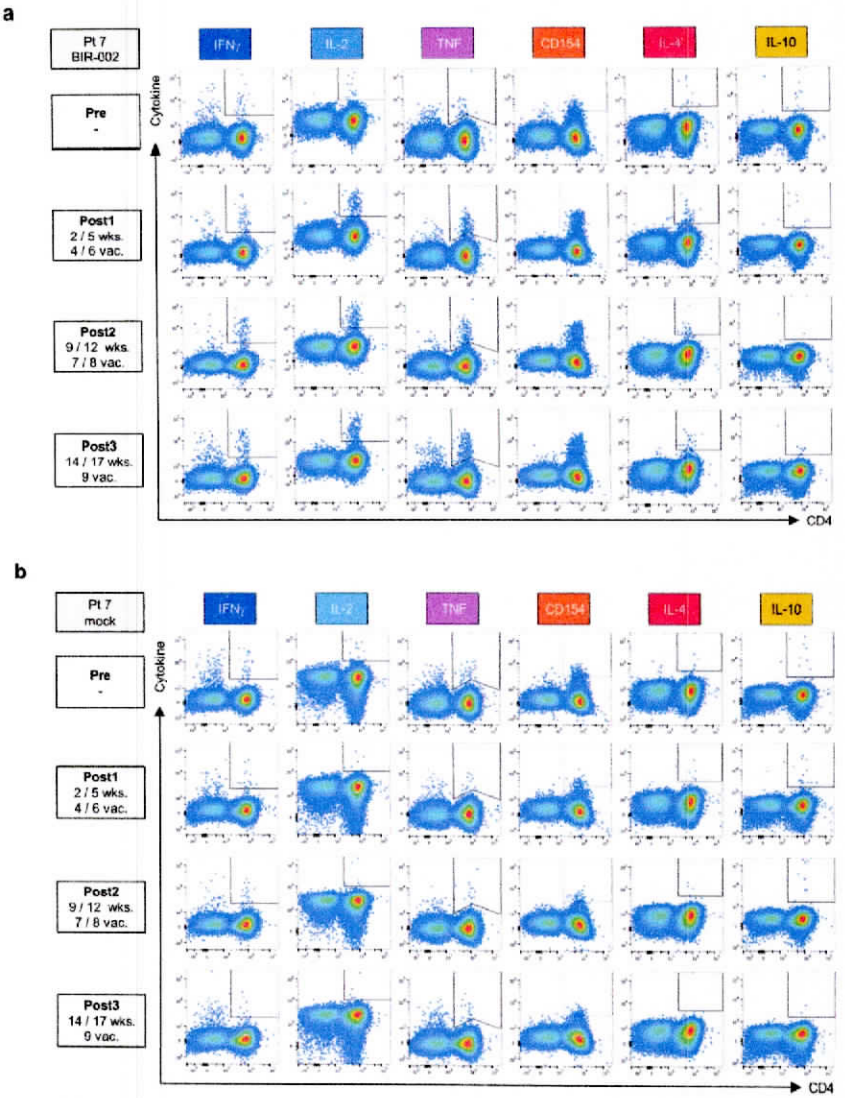

Extended Data Fig. 5 | Ex vivo ICS flow cytometry data for APVAC1-induced CD4$^+$ T cell responses. a, Example flow cytometry data for responses shown in Fig. 2f (CD4$^+$ T cell response of patient 7 to pan-DR antigen BIR-002). IL-5 was negative at all time points (data not shown). **b**, Mock control stimulation for **a**. **a**, **b**, Owing to limited availability of PBMCs, immune response analyses were performed only once per patient. For assays with limited patient materials, see 'Statistical analyses' in Methods.

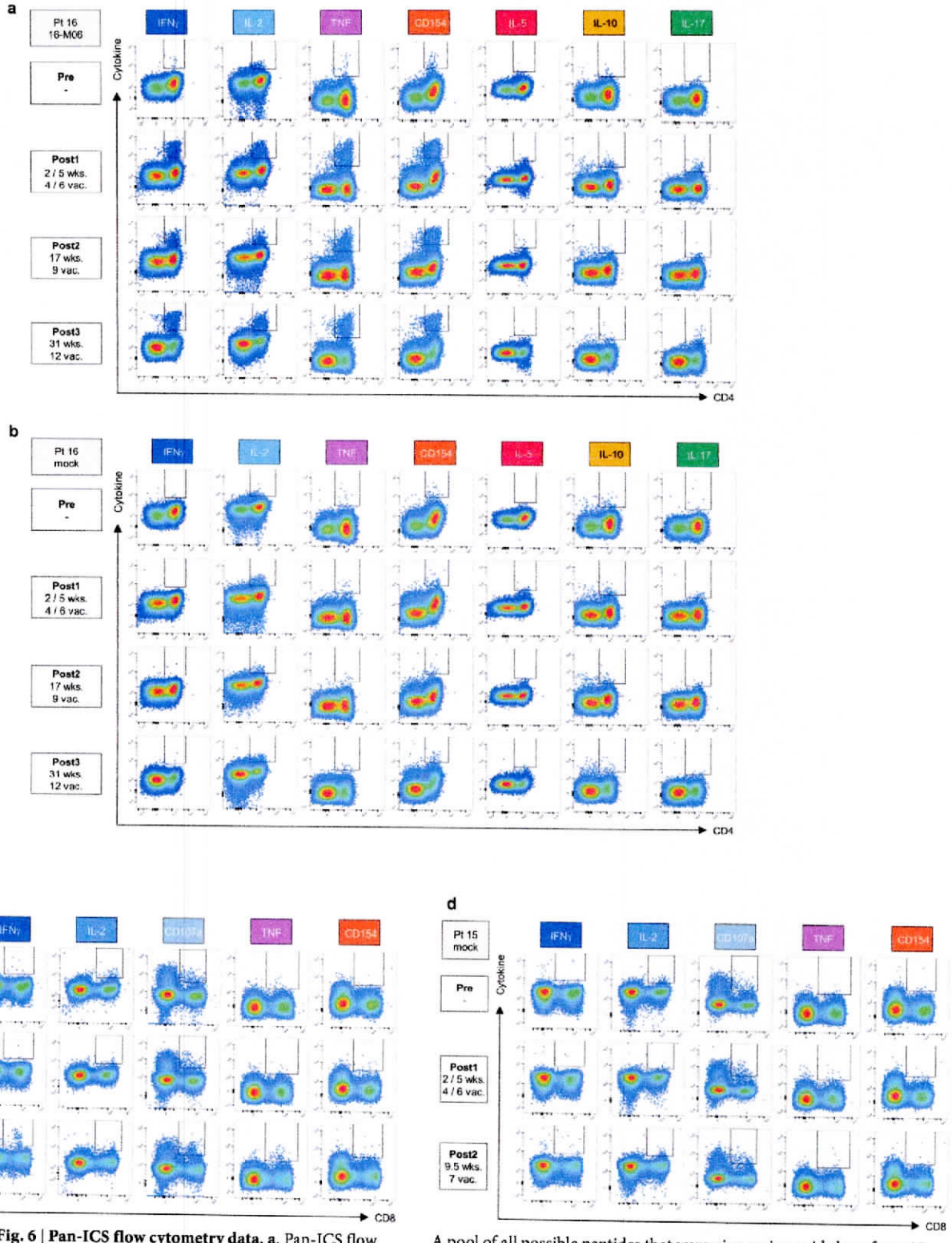

Extended Data Fig. 6 | Pan-ICS flow cytometry data. a, Pan-ICS flow cytometry data for $CD4^+$ T cell response of patient 16 to mutated APVAC2 peptide 16-M06 as summarized in Fig. 4a. Production of indicated cytokines pretreatment (Pre) and at three different post-treatment pools (Post 1 to Post 3) is shown. Post 2 and Post 3 pools originate from the continued vaccination phase (see Fig. 1). Dot plots are gated on $CD8^-$ lymphocytes. Note that the pan-ICS cytokine panel differs from the one used for the ex vivo ICS assay (see Methods). **b**, Mock control stimulation for **a**. **c**, Pan-ICS flow cytometry data for $CD8^+$ T cell response of patient 15 against the mutated APVAC2 peptide 15-M05 as summarized in Fig. 4b. A pool of all possible peptides that were nine amino acids long from 15-M05 was used for read-out. Production of indicated cytokines is shown pretreatment (Pre) and at two different post-treatment pools (Post 1 and Post 2). Dot plots are gated on $CD4^-$ lymphocytes. Note that the APVAC2 analysis time points are not identical to APVAC1 analysis time points owing to the independent start of vaccination (Fig. 1). **d**, Mock control stimulation for **c**. **a**–**d**, Owing to limited availability of PBMCs, immune response analyses were only performed once per patient. For assays with limited patient materials, see 'Statistical analyses' in Methods.

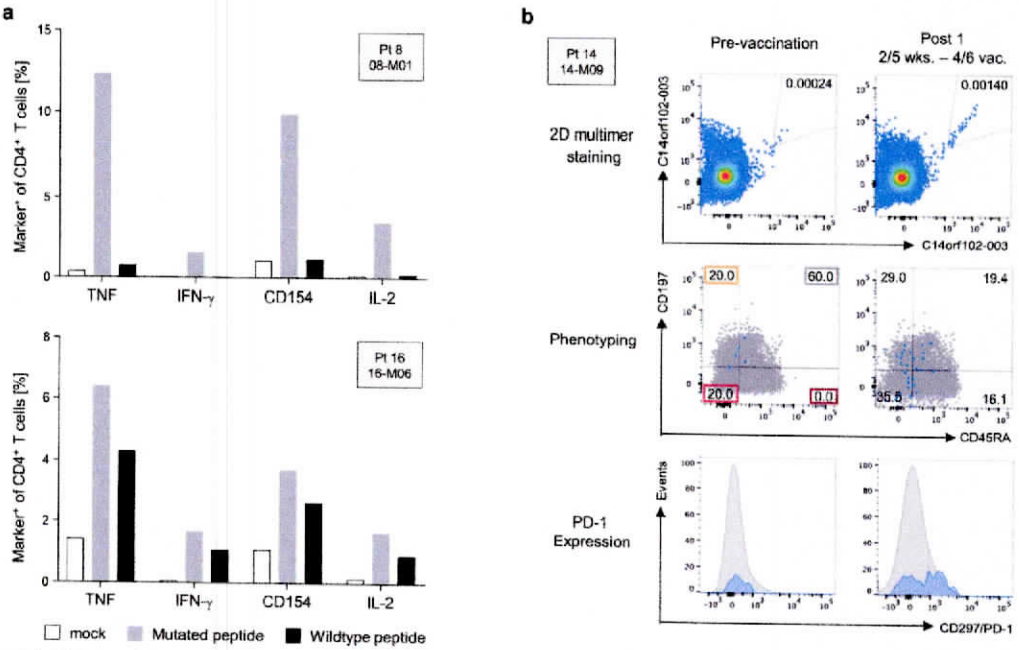

Extended Data Fig. 7 | Additional data on APVAC2-induced, neoepitope-specific immune responses. a, Cross-reactivity of two neoepitope-directed, APVAC2-induced CD4$^+$ T cell responses with the corresponding wild-type peptides was assessed by ICS. Top, response for 08-M01 was specific to the mutated peptide, whereas the response for 16-M06 (bottom) showed considerable cross-reactivity with the wild-type peptide. Owing to limited availability of patient PBMCs, this experiment was performed only once. **b**, Ex vivo 2D multimer data for CD8$^+$ T cell response of patient 14 against the predicted neoepitope HMKVSVYLL contained in the vaccinated peptide 14-M09 as summarized in Fig. 4c. Note that this epitope did not show the highest ranking during APVAC2 selection (underlined in Supplementary Table 4). The pretreatment pool and one post-treatment pool were evaluated. Top, 2D multimer staining. Numbers in plots indicate the frequency of specific cells among total CD8$^+$ T cells. Middle, differentiation phenotyping of specific T cells (blue dots) and total CD8$^+$ T cells (grey dots). Numbers in plots indicate the percentage of specific CD8$^+$ T cells with indicated phenotype (colour code as in Fig. 2a, b). Bottom, PD-1 expression (blue curve, specific CD8$^+$ T cells; grey dots, all CD8$^+$ T cells).

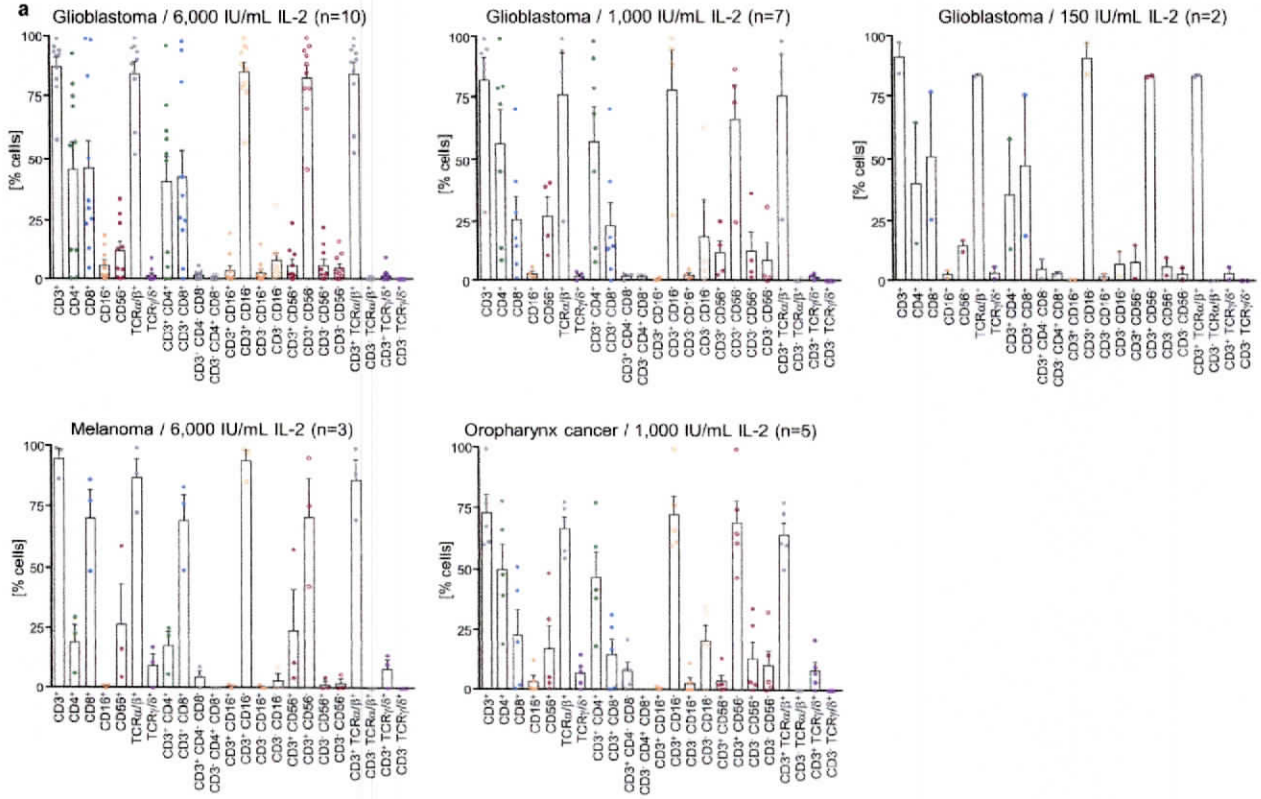

b

	GAPVAC-004						GAPVAC-005				GAPVAC-006	
	Tumor piece 1		Tumor piece 2		Tumor piece 3		Tumor piece 1		Tumor piece 2		1 tumor piece only	
	- OKT3	+ OKT3	- OKT3	+ OKT3	- OKT3	+ OKT3	- OKT3	+ OKT3	- OKT3	+ OKT3	- OKT3	+ OKT3
Starting no. of wells	5	5	5	5	5	5	3	3	12	12	15	15
Harvest	Day 23	Day 18	Day 23	Day 18	Day 23	Day 18	Day 20	Day 15	Day 20	Day 15	Day 19	Day 14
$CD3^+$ lymphocytes [%]	87.3	99.5	89.4	99.6	95.0	99.0	96.5	99.4	97.1	98.7	97.1	98.7
$CD3^+$ $CD4^+$ [%]	40.3	47.5	62.0	49.5	34.2	39.9	18.9	72.3	8.5	68.0	78.3	76.9
$CD3^+$ $CD8^+$ [%]	42.4	50.4	22.7	46.4	57.1	55.5	73.3	25.2	87.4	28.2	14.4	18.3
Cell yield [x10^6]	**0.35**	**71.0**	**0.33**	**50.3**	**0.35**	**22.5**	**6.3**	**93.4**	**21.0**	**72.0**	**3.2**	**76.1**

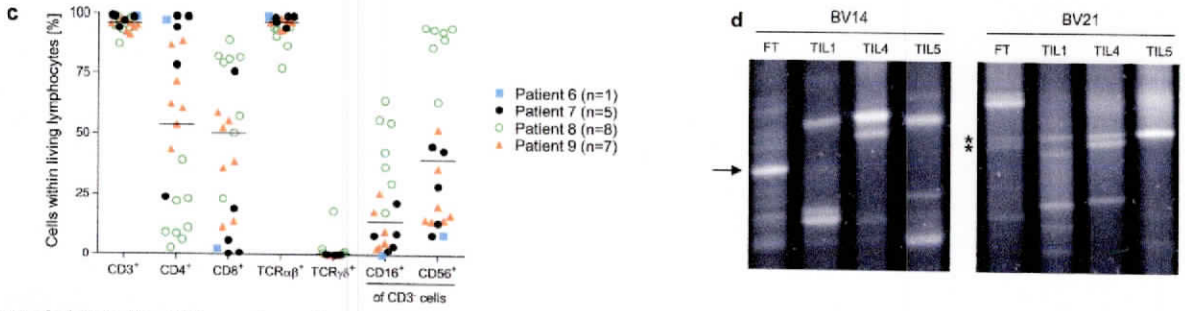

Extended Data Fig. 8 | See next page for caption.

Extended Data Fig. 8 | TIL isolation and expansion in glioblastoma. A harmonized TIL isolation and expansion protocol for glioblastoma specimens was developed in the preclinical phase of the GAPVAC project (see Methods). **a**, Cells were expanded in the presence of recombinant human IL-2 at three concentrations. One centre also performed expansion of melanoma and oropharyngeal TILs for comparison. The number of independent tumours compared across laboratories (preclinical samples) are shown in brackets. Data are mean, s.e.m. and individual values for each cell subset. **b**, Expansion of glioma TILs in the presence or absence of the anti-CD3 antibody OKT3. Indicated number of pieces of tumour obtained from three patients with glioblastoma (outside the GAPVAC-101 trial) were cut in fragments and transferred into 24-well plates with one fragment per well. Fragments were cultured in the absence or presence of 30 ng ml^{-1} anti-CD3 antibody (OKT3). Expanded cells were collected at the indicated days and subjected to phenotyping by flow cytometry. Percentages of total $CD3^+$, $CD4^+$ and $CD8^+$ T cells and total cell yield are indicated. **c**, Compositions of TIL cultures derived at one centre from four different patients (6, 7, 8 and 9) included in the GAPVAC-101 trial. Each dot represents one stain performed either on independent culture wells or after pooling several wells (numbers of independent stainings per patient are indicated). The glioblastoma-derived TILs generally comprised a mixture of $CD4^+$ and $CD8^-$ T cells that varied between individual cultures. Bars indicate the median over all cultures. **d**, Example of TCR clonotype mapping used for a comparative analysis of clonotypes detected ex vivo in the fresh tumour relapse tissue (FT) and in $n = 3$ independent TIL cultures of patient 8. Identical DNA sequences resolve at identical positions in the gel. One prominent BV14 clonotype present in the fresh tissue (arrow) is not amplified in the TIL cultures (left), whereas two of several BV21 clonotypes in the fresh tumour (*) are also detected in the TILs (right). At least $n = 8$ clonotypes per matched set of samples were compared.

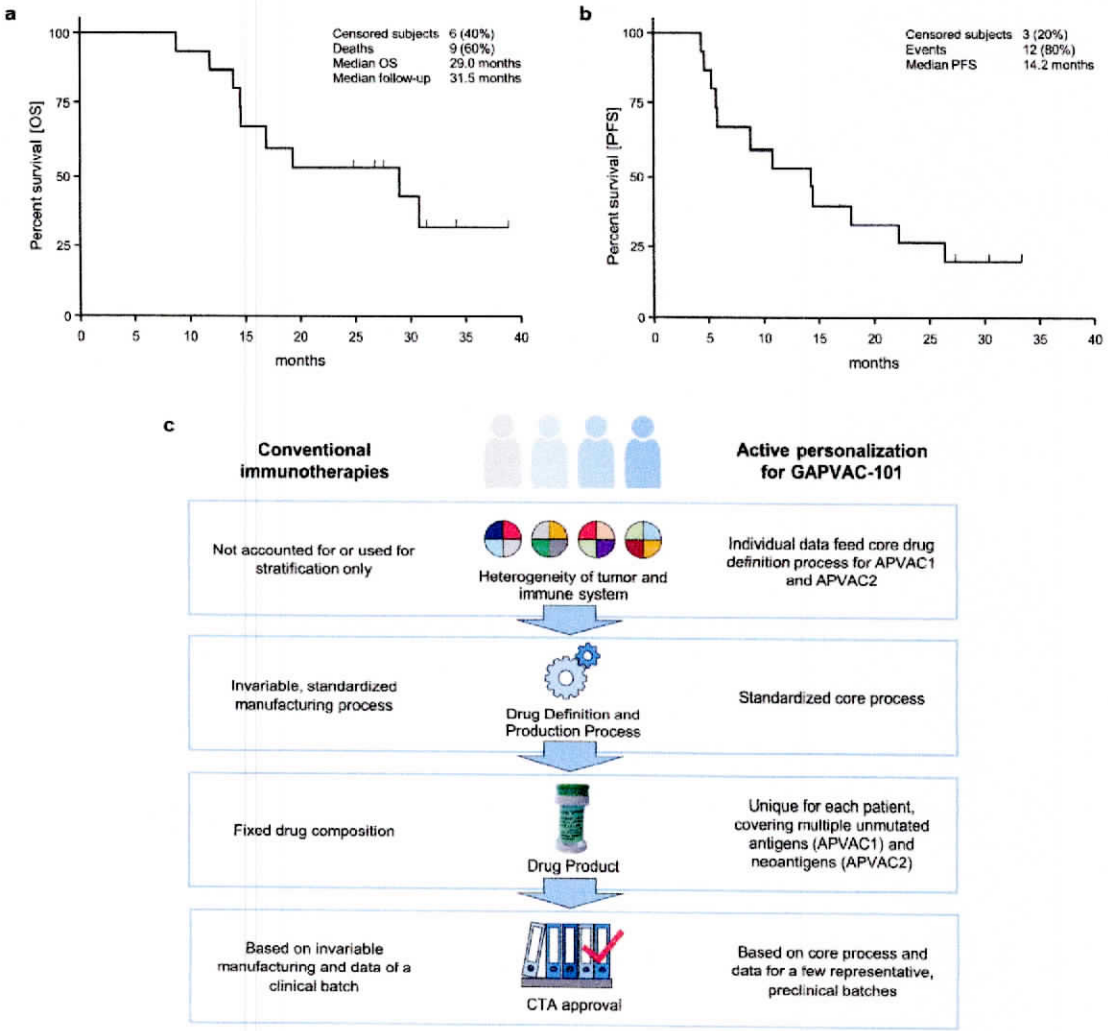

Extended Data Fig. 9 | Survival data for GAPVAC-101 patients. **a**, **b**, Overall survival (OS, **a**) and progression-free survival (PFS, **b**) from diagnosis for all patients that received at least one APVAC vaccination ($n = 15$). Kaplan–Meier estimates of median survival are provided. **c**, Regulatory pathway for active personalized vaccines for GAPVAC-101 compared to conventional immunotherapies. The pathway for clinical trial application (CTA) for GAPVAC-101 was pre-discussed in scientific advice and pre-Investigational New Drug meetings with the German Paul-Ehrlich-Institute (PEI) and the US Food and Drug Administration (FDA), respectively. Key characteristics in the trial approval process were: (1) standardization of a drug composition process based on highly variable, patient-individual biomarker data instead of a fixed drug composition; (2) development of a GMP-compliant core process for manufacturing of variable, personalized multi-peptide compositions instead of an invariable manufacturing process; (3) clinical trial application based on exemplary data from representative preclinical drug substance batches; and (4) provision of certificates of analysis for all APVACs to the authorities on a continuous basis during the trial (twice yearly).

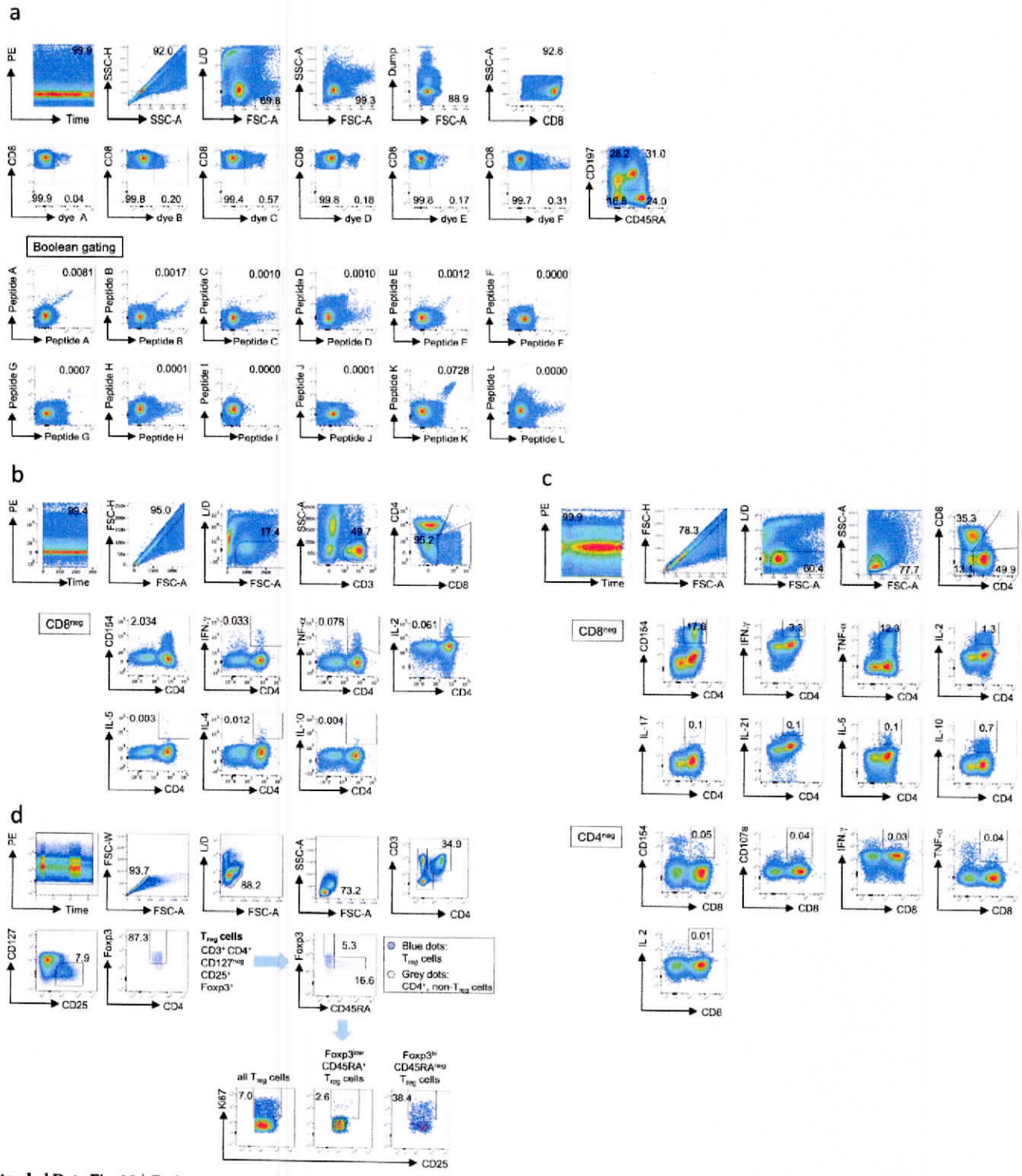

Extended Data Fig. 10 | Gating strategies for flow cytometry assays. **a**, Gating strategy and Boolean gating for ex vivo 2D multimer assay ($CD8^+$ T cell immune response analysis, APVAC1 and APVAC2). **b**, Gating strategy for ex vivo class II ICS assay ($CD4^+$ T cell immune response analysis, APVAC1). **c**, Gating strategy for HLA class I and class II pan-ICS assay ($CD4^+$ and $CD8^-$ T cell immune response analysis, APVAC2). **d**, Gating strategy for T_{reg} cell assay.

nature research

Corresponding author(s): DBPR Nature 2018-05-06359

Reporting Summary

Nature Research wishes to improve the reproducibility of the work that we publish. This form provides structure for consistency and transparency in reporting. For further information on Nature Research policies, see Authors & Referees and the Editorial Policy Checklist.

Statistical parameters

When statistical analyses are reported, confirm that the following items are present in the relevant location (e.g. figure legend, table legend, main text, or Methods section).

n/a	Confirmed	
☐	☒	The exact sample size (*n*) for each experimental group/condition, given as a discrete number and unit of measurement
☐	☒	An indication of whether measurements were taken from distinct samples or whether the same sample was measured repeatedly
☐	☒	The statistical test(s) used AND whether they are one- or two-sided *Only common tests should be described solely by name; describe more complex techniques in the Methods section.*
☐	☒	A description of all covariates tested
☐	☒	A description of any assumptions or corrections, such as tests of normality and adjustment for multiple comparisons
☐	☒	A full description of the statistics including central tendency (e.g. means) or other basic estimates (e.g. regression coefficient) AND variation (e.g. standard deviation) or associated estimates of uncertainty (e.g. confidence intervals)
☐	☒	For null hypothesis testing, the test statistic (e.g. *F*, *t*, *r*) with confidence intervals, effect sizes, degrees of freedom and *P* value noted *Give P values as exact values whenever suitable.*
☒	☐	For Bayesian analysis, information on the choice of priors and Markov chain Monte Carlo settings
☐	☒	For hierarchical and complex designs, identification of the appropriate level for tests and full reporting of outcomes
☒	☐	Estimates of effect sizes (e.g. Cohen's *d*, Pearson's *r*), indicating how they were calculated
☐	☒	Clearly defined error bars *State explicitly what error bars represent (e.g. SD, SE, CI)*

Our web collection on statistics for biologists may be useful.

Software and code

Policy information about availability of computer code

Data collection	Clinical data collection and management was carried out using SAS (version 9.3; SAS Institute, Cary, NC) after double-data entry from a paper CRF. Ex vivo multimer data, pan-ICS and ex vivo ICS data were acquired on a BD LSRII SORP flow cytometer. ELISpot data were acquired with an ImmunoSpot Series 6 ELISpot Reader (C.T.L. Europe, Germany). TIL functional data (flow cytometry) were acquired on an LSR Fortessa SORP equipped with Diva v6.1.2. Treg flow cytometer data were collected on a BD FACSCanto II and analysed using FlowJo software version 10. MS data have been acquired on an Orbitrap Velos and Orbitrap fusion (ThermoFisher). RNA microarray data were acquired by Affymetrix Human Genome (HG) U133 Plus 2.0 oligonucleotide microarrays using an Affymetrix GeneChip Scanner 3000.
Data analysis	Where applicable, data were reported as the median (indicating the range from minimum to maximum value occurred) and arithmetic mean ± standard deviation, as specified (R software package, 3.4.1). Dichotomous variables were evaluated by Fisher's exact test while continuous variables were compared by two-sided t test or Mann-Whitney U test, as indicated. OS and PFS (both calculated from primary tumour diagnosis) were assessed by Kaplan-Meier analysis using Prism 7 (GraphPad Software Inc., CA). An independent data safety monitoring board oversaw the study. Mutation analysis used a software pipeline employing: bwa, bowtie, Immune Epitope Database (IEDB) T-cell prediction tools (version 2.5, IEDB-recommended mode), primer3 software, BLAT. Patient PBMC were limited in this study. If not stated otherwise and owing to limited sample availability, immune response assessments could only be performed once and were not repeated. As detailed in the sections for ex vivo 2D multimer, ex vivo ICS and pan-ICS, various internal and external controls were included and per assay type, all patient assays were done with the same batches of critical reagents (e.g. staining antibodies). Further, all patient assays were performed according to detailed standard operating procedures.

Ex vivo multimer, and ICS, pan-ICS data,Treg flow cytometer data and TIL functional data were analysed using FlowJo software version 10 (Tree Star, Ashland, USA).
LC-MS/MS data were acquired on an Orbitrap Velos or Orbitrap Fusion (Thermo Scientific).
mRNA expression microarray data was evaluated by the Affymetrix GeneChip Command Console (AGCC) software.

For manuscripts utilizing custom algorithms or software that are central to the research but not yet described in published literature, software must be made available to editors/reviewers upon request. We strongly encourage code deposition in a community repository (e.g. GitHub). See the Nature Research guidelines for submitting code & software for further information.

Data

Policy information about availability of data

All manuscripts must include a data availability statement. This statement should provide the following information, where applicable:

- Accession codes, unique identifiers, or web links for publicly available datasets
- A list of figures that have associated raw data
- A description of any restrictions on data availability

The authors declare that [the/all other] data supporting the findings of this study are available within the paper [and its supplementary information files]. The data will also be publicly available at the Consortium's homepage (www.gapvac.eu). This is our own policy and following the EU grant requirements.

Field-specific reporting

Please select the best fit for your research. If you are not sure, read the appropriate sections before making your selection.

☒ Life sciences ☐ Behavioural & social sciences ☐ Ecological, evolutionary & environmental sciences

For a reference copy of the document with all sections, see nature.com/authors/policies/ReportingSummary-flat.pdf

Life sciences study design

All studies must disclose on these points even when the disclosure is negative.

Sample size	For the phase I safety question 3+3 patients would have been sufficient. As the trial aimed at showing feasibility and biological mechansims of action (immunogenicity), we calculated 15 evaluable patients to be sufficient to claim feasibility and to generate a meaningful dataset based on immunogenicity as below: Prospectively and based on previous experience with the off-the-shelf vaccines IMA901 and IMA910 heading for a minimal multi-TUMAP response rate of 40% was considered a reasonable target for the personalized APVAC approach. Calculating with 15 patients evaluable for APVAC1 class I peptides and assuming an observed multi-TUMAP responder rate of 67% (10/15 patients; CI0.95: 38-88%), the probability to see that effect if the true multi-TUMAP response rate really is equal to the target value of 40% would be p=0.061 (two-sided exact binomial test; R software package, version 3.0.2), i.e. a true multi-TUMAP responder rate greater than 40% would be very likely (probability 93.9%). In the data analysis, the true multi-TUMAP responder rate was much higher. Thus, this endpoint was clearly met, justifying also the set sample size.
Data exclusions	No data were excluded, but patient screened and tested for the trial did not necessarily reach the stage of treatment as detailed in Suppl. Figure 1.
Replication	All clinical data derive their relevance from the treatment of multiple patients; we deemed 16 patients included into the trial as sufficient to show feasibility. Replication of analysis of patient samples was in most cases not possible due to limited amount of patient specimens. Methods for analysis of patient samples where standardized and highly controlled (e.g. immune response analysis, NGS) according to accepted standards in the field. Where applicable, number of replicates are indicated. Variation has been adressed by the number of patients.
Randomization	The trial aims at showing biological effects, not superiority over a standard. Given the immune monitoring being the main outcome, these data would not benefit from randomization but negative controls, which are included. Variation has been adressed by the number of patients.
Blinding	The clinical evaluation regarding toxicity was non-blinded. Blinding would not enhance awareness in this phase I trial. The clinical efficacy data (MRI) were assessed centrally and blinded for the stage and kind of therapy. The translational/immune monitoring data were blinded to any clinical treatment.

Reporting for specific materials, systems and methods

Materials & experimental systems

n/a	Involved in the study
☐	☒ Unique biological materials
☐	☒ Antibodies
☒	☐ Eukaryotic cell lines
☒	☐ Palaeontology
☒	☐ Animals and other organisms
☐	☒ Human research participants

Methods

n/a	Involved in the study
☒	☐ ChIP-seq
☐	☒ Flow cytometry
☐	☒ MRI-based neuroimaging

Unique biological materials

Policy information about availability of materials

Obtaining unique materials: The APVAC 1 and APVAC2 are commercially available at providers for synthethic peptides and sequences are provided. Since APVAC2 has been academically produced according to specific (individual) mutations, sharing material has limited value, but all data for repetition are public.

Antibodies

Antibodies used: All used antibodies are commercially available and have been specified in the Online Methods part with clone, provider and flurochrom (if applicable). In detail:

Ex vivo
CD8-FITC (SK1, Biolegend, cat. 344704, lot B153198, 1:200)
CD279/PD-1-BV786 (EH12.1, BD, cat. 563789, lot 5253586, 1:20)
CD197/CCR7-PE-CF594 (150503, BD, cat. 562381, lot 5295853, 1:20)
CD45RA-AF700 (HI100, Biolegend, cat. 304120, lot B195192, 1:500)
CD4-PE-Cy5 (RPA-T4, BD, cat. 555348, lot 5037589, 1:80)
CD14-PE-Cy5 (61D3, eBioscience, cat. 15-0149-42, lot E17234-103, 1:750)
CD16 (3G8, BD cat. 555408, lot 4355578, 1:450)
CD19 (HIB19, BD, cat. 555414, lot 4357815, 1:300) antibodies for dump channel (all PE-Cy5)

Ex vivo HLA class II ICS assay:
CD8-BV570 (RPA-T8, Biolegend, cat. 301038, lot B204278, 1:100)
CD3-BV711 (OKT3, Biolegend, cat. 317328, lot B197951, 1:340)
CD4-BV605 (OKT4, Biolegend, cat. 317438, lot B196540, 1:130)
CD154-FITC (TRAP1, BD, cat. 555699, lot 4293606, 1:500)
IFN-gamma-PE-Cy7 (4S.B3, BD, cat. 557844, lot 5190774, 1:1200)
IL-2-BV510 (MQ1-17H12, Biolegend, cat. 500338, lot B204028, 1:65)
IL-4-BV421 (MP4-25D2, Biolegend, cat. 500826, lot B201458, 1:480)
IL-5-PE (JES1-39D10, BD, cat. 559332, lot 5051710, 1:10)
IL-10-APC (JES3-9D7, Miltenyi, cat. 130-096-042, lot 5160615335, 1:20)
TNF-alpha-AF700 (MAb11, BD, cat. 557996, lot 5225619, 1:225).

Pan-ICS
CD107a-FITC (H4A3, BD, cat. 555800, lot 6266751, 1:60)
CD8-BV605 (SK1, Biolegend, cat. 344742, lot B231678, 1:500)
CD4-BV785 (RPA-T4, BioLegend, cat. 300554, lot B229165, 1:2000)
CD154-BV421 (TRAP1, BD, cat. 563886, lot 6280762, 1:50)
IFN-gamma-PE-Cy7 (4S.B3, BD, cat. 557844, lot 6251991, 1:1000)
IL-2-BV510 (MQ1-17H12, Biolegend, cat. 500338, lot B222707, 1:100)
IL-5-PE (JES1-39D10, BD, cat. 559332, lot 6112747, 1:30)
IL-10-BV650 (JES3-9D7, BD, cat. 564051, 7037872, 1:10)
IL-17A-BV570 (BL168, BioLegend, cat. 512324, lot B198270, 1:100)
IL-21-APC (3A3-N2, BioLegend, cat. 513008, lot B220480, 1:15)
TNF-alpha-AF700 (MAb11, BD, cat. 557996, lot 7034802, 1:300)

Functional TIL testing
CD4-APC-Cy7 (BD, 1:100, clone RPA-T4/ cat n° 55787)
CD8-PECy7 (Beckman Coulter, 1:400; clone SFCI21Thy2D3 cat n° 737661)
CD3-BV711 (Biolegend, 1:67; clone OKT3 cat n° 317317)
anti-CD154 APC (BD, 1:12.5; clone TRAP1 cat n° 555702
anti-IFN-gamma FITC (BD, 1:200; clone B27 cat n° 554700)
anti-IL-2 PE (BD, 1:130; clone MQ1-17H12 cat n° 554566)
TNF Pacific Blue (Biolegend, 1:120; clone MAb11 cat n° 502920

Treg assays
CD3-pacific blue (clone SK7, Biolegend; 1:40; Cat 344823/4, Lot B214022/B214021)
CD4-APC.Cy7 (clone SK3, Biolegend, 1:40 (Cat 344615/6, Lot B212646)
CD25-APC (clone M-A251, Biolegend; 1:20; Cat 356110, Lot B206326)

	CD45RA-PerCP.Cy5.5 (clone HI100, Biolegend; 1:40; Cat 304121/2, Lot B213967/B213966) CD127-PE.Cy7 (clone HIL-7R-M21, BD; 1:20; Cat 560822, Lot 6141805) FoxP3-Alexa488 (clone 259D/C7, BD; 1:5; Cat 560047, Lot 6051566) Ki67-PE (clone Ki67, Biolegend; 1:20; Cat 350504, Lot B180057/B222354)
Validation	Product Data Sheets are available for all used antibodies containing information about intended use and applicability for human cells, specificity, and cross-reactivity. Staining panels have been established before use with patient material and antibodies have been titrated for optimal performance.

Human research participants

Policy information about studies involving human research participants

Population characteristics	Inclusion criteria are integrated; the main eligibility criteria include: newly diagnosed glioblastoma, adult, no prior therapy except surgery, sufficient tumor tissue and option to undergo leukapharesis; eligibility for standard radiochemotherapy, into which our experimental treatment would be integrated. HLA A02 or A24 positivity. Absence of immunedefects or immunosuppressive therapies.
Recruitment	All patients in all participating sites have been informed on the trial pre- or postoperatively. The patient information followed a two-stage process as HLA haplotype was an inevitable prerequisite. The intended bias is not likely possible.

Flow Cytometry

Plots

Confirm that:

☒ The axis labels state the marker and fluorochrome used (e.g. CD4-FITC).

☒ The axis scales are clearly visible. Include numbers along axes only for bottom left plot of group (a 'group' is an analysis of identical markers).

☒ All plots are contour plots with outliers or pseudocolor plots.

☒ A numerical value for number of cells or percentage (with statistics) is provided.

Methodology

Sample preparation	Patient PBMC were isolated within 8 h from venipuncture from patients' sodium heparin blood by standard Ficoll-Hypaque density gradient centrifugation using fully standardized procedures. Cells were cryopreserved in serum-free medium and stored in the gas phase of liquid nitrogen prior to central, standardized assessment of immune responses.
Instrument	BD LSRII SORP flow cytometer
Software	FlowJo software version 10.1 (Tree Star, Ashland, OR, USA)
Cell population abundance	No flow-based sorting steps involved.
Gating strategy	Gating strategies for all four flow cytometry panels are provided in Extended Data Fig. 10.

☒ Tick this box to confirm that a figure exemplifying the gating strategy is provided in the Supplementary Information.

Magnetic resonance imaging

Experimental design

Design type	Anatomical/structural Imaging for tumor assessment
Design specifications	Standard protocol according to Ellingson et al. Neuro Oncol 2016. and RANO criteria (Wen et al. JCO 2010)
Behavioral performance measures	N/A

Acquisition

Imaging type(s)	Structural
Field strength	3 Tesla
Sequence & imaging parameters	Images were acquired in the routine clinical workup using a 3 Tesla MR system (Magnetom Verio/Trio TIM, Siemens Healthcare, Erlangen, Germany) with a 12- or 16-channel head-matrix coil. Briefly, the protocol included T1-weighted 3D MPRAGE images both before (T1) and after (cT1) administration of a 0.1 mmol/kg dose of gadoterate meglumine (DOTAREM, Guerbet, France) as well as axial FLAIR and axial T2-w images. The standard MRI protocol included axial T1-weighted imaging (TR, 400 ms; TE, 15 ms; section thickness, 5 mm; FOV, 230 mm) or alternatively a T1-weighted 3D

MPRage (TR, 1740 ms; TE, 3.45 ms; section thickness, 1.0 mm; FOV, 250 mm) without and with contrast media (Gadovist, Bayer, Leverkusen, Germany, 0.1mmol/kg); T2-weighted imaging (TR, 4890 ms; TE 85 ms; section thickness, 5 mm; FOV, 230 mm), FLAIR (TR, 8500 ms; TE, 85 ms; TI, 2400 ms; section thickness, 5 mm; FOV, 230 mm).

Area of acquisition: Whole brain scan until C2 in the spine.

Diffusion MRI ☐ Used ☒ Not used

Preprocessing

Preprocessing software: N/A

Normalization: *If data were normalized/standardized, describe the approach(es): specify linear or non-linear and define image types used for transformation OR indicate that data were not normalized and explain rationale for lack of normalization*

Normalization template: *Describe the template used for normalization/transformation, specifying subject space or group standardized space (e.g. original Talairach, MNI305, ICBM152) OR indicate that the data were not normalized.*

Noise and artifact removal: *Describe your procedure(s) for artifact and structured noise removal, specifying motion parameters, tissue signals and physiological signals (heart rate, respiration).*

Volume censoring: *Define your software and/or method and criteria for volume censoring, and state the extent of such censoring.*

Statistical modeling & inference

Model type and settings: N/A

Effect(s) tested: Analysis of tumor response according to RANO criteria

Specify type of analysis: ☐ Whole brain ☐ ROI-based ☐ Both

Statistic type for inference (See Eklund et al. 2016): N/A

Correction: *Describe the type of correction and how it is obtained for multiple comparisons (e.g. FWE, FDR, permutation or Monte Carlo).*

Models & analysis

n/a	Involved in the study
☐	☐ Functional and/or effective connectivity
☐	☐ Graph analysis
☐	☐ Multivariate modeling or predictive analysis

Functional and/or effective connectivity: N/A

Graph analysis: *Report the dependent variable and connectivity measure, specifying weighted graph or binarized graph, subject- or group-level, and the global and/or node summaries used (e.g. clustering coefficient, efficiency, etc.).*

Multivariate modeling and predictive analysis: *Specify independent variables, features extraction and dimension reduction, model, training and evaluation metrics.*